From wastepaper to functional materials: recycling of cellulose through “green” aqueous solvents

Camelia Oliva

Department of Food Science & Agricultural Chemistry, McGill University, Montreal

June 2020

“A thesis submitted to McGill University in partial fulfillment of the requirements of the degree of Masters of Science in Food Science & Agricultural Chemistry”

Table of Contents

List of Figures

Chapter 2

Chapter 3

Chapter 4

List of Tables

Chapter 4

Abstract

Cellulose is the most abundant biopolymer in nature. Cellulose is renewable, biocompatible, biodegradable, and non-toxic. However, strong inter- and intra-molecular hydrogen bonds as well as hydrophobic interactions exist among cellulose molecules. Consequently, it is rendered insoluble in most commonly used inorganic/organic solvents. The traditional cellulose solvent from the viscose route causes serious environmental pollution, so many efforts have been made to develop novel cellulose solvents and study their dissolution mechanisms. Several solvent systems have been reported in recent years, which can be classified as acidic aqueous systems, alkali/urea aqueous systems, ionic liquid systems, and mixed solvent systems. Various cellulose-based functional materials, such as films, hydrogels, and aerogels, can be regenerated from these solvent systems, and have attracted more and more attention. In Chapter 2, the recent development of cellulose-based materials with potential applications in food related fields was summarized, including food packaging, food thermal insulation, encapsulation of micronutrients and nutraceuticals, water treatments, and food agriculture. In Chapter 3, waste paper, a major contributor to municipal and industrial waste, was converted into value-added cellulose films through rapid dissolution in -20$_o$C H_2SO_4 aqueous solution. Two types of waste paper, office paper and cardboard, could be dissolved within 210 s, and their crystalline structures transformed to type II during dissolution and regeneration. The regenerated office paper films were transparent, and exhibited excellent mechanical properties (tensile strength: 77.55±6.52 MPa, elongation at break: 2.67±0.30%, and Young’s modulus: 5451.67±705.23 MPa), which were comparable to those of cellulose films prepared from spruce pulp in the same solvent. Moreover, the regenerated films were a promising matrix to load antimicrobial compounds, and thus, inhibited the growth of pathogenic bacteria. In Chapter 4, waste office paper was recycled by dissolving in NaOH/urea aqueous solution and then regenerated into cellulose hydrogels as a biodegradable matrix for controlled releasing fertilizer, and at the same time, retaining water for dryland agriculture. The structure and properties of obtained cellulose hydrogels were studied by ATR-FTIR, XRD, SEM, re-swelling test, and fertilizer release test. The results revealed that, after pre-hydrolysis, waste office paper could be partially dissolved in NaOH/urea aqueous solution at -12.6 $_{o}$C within 15 min, and form cellulose beads after regeneration via simple drop-wise syringe extrusion in a 10 wt% sulfuric acid coagulation bath. The crystalline structure of cellulose changed from cellulose type I to cellulose type II during dissolution and regeneration. The obtained cellulose beads had porous structure and could successfully load fertilizer (freeze-dried beads: 143.3 ±8.52 mg/g and oven-dried beads: 127.9 ±2.56 mg/g). Moreover, the hydrophilic matrix of cellulose hydrogels enabled the absorption of water in their three-dimensional network. Two different drying methods, namely freeze drying and oven drying, did not show a significant effect on the amounts of N-P-K fertilizer released from the cellulose beads (freeze-dried beads: N: 56.8 ±3.92 mg/g, P: 49.7±3.82 mg/g and K: 36.8±1.38 mg/g and oven-dried beads: N: 49.7±0.726 mg/g, P: 44.1±1.70 mg/g and K: 34.1±1.11 mg/g). However, the re-swelling ratio of freeze-dried beads (415.62±18.13 %) was evidently higher than that of oven-dried beads (224.16±5.51%). Overall, this research demonstrated a “green” method to recycle waste paper into biodegradable functional materials with potential applications in food packaging and agriculture.

Résumé

La cellulose est un bio-polymère qui est le plus abondant dans la nature. Ce bio-polymère est renouvelable, biocompatible, biodégradable, compostable et non-toxique à l'environnement.

Par contre, dans la structure du polymère il y a de fortes liaisons hydrogène inter- et intramoléculaires et d'interactions hydrophobes. Par conséquent, la cellulose est insoluble dans les solvants inorganiques/ organiques communs. Le solvant traditionnel qui est utilisé, en industrie, cause de sérieuses pollutions de l'environnement. Alors, beaucoup d'efforts, plus récents, ont été fait dans la recherche pour développer de nouveaux solvants alternatifs et plus écologiques. Ils peuvent être classifiés comme les solvants de systèmes : acides aqueux, alcali/urée aqueux, de liquides ioniques et solvants mixtes. De plus, divers matériaux fonctionnels basés de celluloses peuvent être régénérés avec ces solvants alternatifs comme de films de celluloses de plastiques, des hydrogels et des aérogels, et cela attire de plus, en plus l'attention. Dans le chapitre 2, une revue de littérature résume les développements des matériaux fonctionnels basés de celluloses avec le potentiels d'applications reliés dans le domaine agro-alimentaire comme : l'emballage d'alimentations, isolations thermique des aliments, l'encapsulation de micronutriments et de nutraceutiques, les traitements d'eaux et l'agricultures alimentaires. Dans le chapitre 3, des vieux papiers (riche en ressources naturelles de celluloses) qui sont jetés, contribue en-grosse masses, aux déchets industriels et municipaux et ils ont étés régénérés en films de celluloses de plastiques avec le solvant pré-refroidi (-20$_{o}$C) aqueux acide sulfurique. Deux types de vieux papiers ont étés utilisés (papier de bureau et de cartons), ou ils peuvent se dissoudre dans le solvant pré-refroidi aqueux acide sulfurique, en 210 sec., et leurs structures cristallines ont été transformés en cellulose de type II durant la dissolution et la régénération. Les papiers de bureau régénéré en films de plastiques étaient transparent et avaient d’excellents propriétés mécaniques (la résistance à la traction: 77.55±6.52 MPa, d’allongement à la rupture: 2.67±0.30% et Module d’Young: 5451.67±705.23 MPa) qui étaient comparable aux films de plastiques préparés de pulpe d’épinette du même solvant. De plus, ces films de cellulose de plastiques avaient une matrice prometteuse pour charger avec des composés antimicrobiens et ainsi ont démontrés une inhibition de croissance des bactéries pathogènes. Dans le chapitre 4, des vieux papiers de bureau ont étés recyclés par leurs dissolution dans le solvant aqueux de NaOH/urée et régénérés en hydrogels de celluloses comme une matrice pour un contrôle-libération des fertilisants, et en-même-temps, elle sert comme réservoir d’eaux pour humidifier avec contrôle les terres arides pour l’agriculture. La structure et les propriétés des hydrogels de cellulose obtenus ont été étudiées par ATR-FTIR, XRD, SEM, test de regonflement et test de libérations de fertilisants. Les résultats ont révélés, qu’après la pré-hydrolyse, les vieux papiers de bureau peuvent être partiellement dissous dans le solvant aqueux NaOH/urée à -12.6$_{o}$C en 15 min, pour former des billes de cellulose après régénération par simple injection à la seringue dans un bain de coagulation à 10 % de la masse d'acide sulfurique. La structure cristalline de cellulose a changé de cellulose de type I a cellulose de type II durant la dissolution et régénération. Les billes en celluloses obtenus avaient une structure poreuse et peuvent bien se faire charger avec des fertilisants (billes lyophilisées: 143.3 ±8.52 mg/g et billes séchées-au-four: 127.9 ±2.56 mg/g). De plus, la matrice hydrophile des hydrogels de cellulose a permis l'absorption d'eau dans leur réseau tridimensionnel. Deux méthodes de séchage différentes ont été fait, la lyophilisation et le séchage au four, et ils n'ont pas montré d'effet significatif sur les quantités des fertilisants N-P-K libérées par les billes de cellulose (billes lyophilisées: N: 56.8 ±3.92 mg/g, P: 49.7±3.82 mg/g and K: 36.8±1.38 mg/g et billes séchées-au-four: N: 49.7±0.726 mg/g, P: 44.1±1.70 mg/g and K: 34.1±1.11 mg/g). Cependant, le taux de regonflement des billes

lyophilisées (415.62 ± 18.13%) était évidemment supérieur à celui des billes séchées-au-four (224.16 ± 5.51%). Dans l'ensemble, cette recherche a démontré une méthode «verte» pour recycler les vieux papiers en matériaux fonctionnels, biodégradables et ayant des applications potentielles pour l'emballage alimentaire et l'agriculture.

Contribution of Authors

This thesis consists of five chapters as follows: Chapter 1 is a general introduction that includes a brief overview of the recent related work in the literature and states the objectives of the research presented in the thesis. Chapter 2 is a detailed review of the recent development of cellulose materials regenerated from different solvent systems for food applications. Chapter 3 presents the sulfuric acid aqueous solvent enabling the rapid recycling of waste paper into antimicrobial packaging, and has been published in the journal *Carbohydrate Polymers*. Chapter 4 reports the recycling of wastepaper into cellulose hydrogels for water and fertilizer savings in dryland agriculture, and is to be submitted for publication in the *Journal of Agricultural and Food Chemistry*. Finally, Chapter 5 presents an overall conclusion of the thesis as well as some recommendations for future research.

The present author, Camelia Oliva, was responsible for the experimental work, data acquisition and analysis, and the writing of the thesis. Dr. Yixiang Wang was the thesis supervisor and had direct advisory for all the experimental design and the manuscripts. In Chapter 3, Dr. Weijuan Huang participated in sample characterization and data acquisition, and edited the manuscript before submission. Ms. Souhaïla El Badri carried out the preliminary experiment. Ms. Maria Ai Lan Lee conducted the antimicrobial test. Dr. Jennifer Ronholm provided the suggestion about the antimicrobial test and edited the manuscript. Dr. Lingyun Chen supported the sample characterization and edited the manuscript before submission

Acknowledgements

I would like to first give my sincerest appreciation towards my supervisor Dr. Yixiang Wang for providing me with the utmost guidance, expertise, support, resources and lab facilities to carry-on my research. I would also like to extend my gratitude towards my committee member Dr. Benjamin K. Simpson for providing me with some resources and lab facilities to carry-on my research. A special thank-you to both these professors for truly making this an enriching learning experience.

I would like to thank my co-authors (Dr. Weijuan Huang, Ms. Souhaïla El Badri, Ms. Maria Lee, Dr. Jennifer Ronholm and Dr. Lingyun Chen) who have assisted me in publishing my very first manuscript.

In addition, I would like to acknowledge Dr. Chandra Madramootoo (Department of Bioresource and Engineering) for including me in his MSSI funding award he and my supervisor won.

Further acknowledgements would have to be towards some of my lab mates (Paola Sully and Shuting Huang) for their encouragement, assistance and friendship.

Finally, I would like to acknowledge and thank my family, my significant other and friends for their unconditional psychological and emotional support.

List of Abbreviations

AGU:	D-Anhydroglucopyranose Unit
AmimCl:	1-allyl-3-methylimidazolium chloride
ANOVA:	Analysis of Variance
ATR-FTIR:	Attenuated Total Reflectance-Fourier Transform Infra-Red
[Bmim][Cl]:	1-butyl-3-methylimidazolium
13C-NMR:	Carbon-13 Nuclear Magnetic Resonance
CCNMs:	Cellulose Fibers/ Cellulose Nanofibers Macrogels
CF:	Commercial Fertilizer
CFU:	Colony Forming Unit
CNFs:	Cellulose Nanofibers
CP:	Cardboard Paper
DMF:	Dimethylformamide
DMI:	1,3-dimethyl-2-imidazolidinone
DMSO:	Dimethyl-sulfoxide
DSC:	Differential Scanning Calorimetry
EmimAc:	Ethy1-3-methylimidazolium acetate
[Emim][DEP]:	1-ethyl-3-methylimidazolium phosphate
EO:	Essential Oil
FAO:	Food Agricultural Organization
FD:	Freeze Dried
FT-IR:	Fourier Transform Infra-Red
GHG:	Green House Gas

H_2SO_4:	Sulfuric Acid
HP:	Hydrolyzed Paper
IL:	Ionic Liquid
LiCl/DMAc:	Lithium Chloride /N,N-Dimethylacetamide
LiOH/urea:	Lithium hydroxide/urea
MCC:	Micro-Crystalline Cellulose
MFC:	Micro-Fibrillated Cellulose
MH NPs:	Magnesium Hydroxide Nanoparticles
N-P-K:	Nitrogen-Phosphorus-Potassium
NaOH/Urea:	Sodium Hydroxide/Urea
NMR:	Nuclear Magnetic Resonance
OD:	Oven Dried
OP:	Office Paper
PHFs:	Porous Hybrid Fibers
PMMA:	Poly(Methyl Methacrylate)
RC:	Regenerated Cellulose
RC/ PEO:	Regenerated Cellulose/ Poly(Ethylene Oxide)
RC/ATT:	Regenerated Cellulose/ Attapulgite
RCB:	Regenerated Cardboard
RMP:	Regenerated Mixed Paper
ROP:	Regenerated Office Paper
RSR:	Re-Swelling Ratio
SEM:	Scanning Electron Microscope

SGF:	Simulated Gastric Fluid
SIF:	Simulated Intestinal Fluid
TBAH:	Tetra-Butyl-Ammonium Hydroxide
TEM:	Transmission Electron Microscope
UV-vis:	Ultraviolet-visible
W:V:	Weight: Volume
WCFs:	Waste Cotton Fabrics
XRD:	X-Ray Driffraction
ZNC:	ZnO-Cellulose Nanocomposite
ZnO:	Zinc Oxide

Chapter 1. Introduction

1.1 General Introduction

The non-degradable plastic materials have created a rubbish problem that now pollutes every corner of the world. It has directly threatened human being's health, development, and even survival. Thus, there is currently an urgent requirement to develop biodegradable functional materials (Genga et al., 2014). Cellulose is a ubiquitous structural polymer that confers its mechanical properties to higher plant cells. It constitutes approximately 33% of plants, 50% of wood, and 90% of cotton, so it is the most abundant natural polymer with good biocompatibility, biodegradability, and compostability to environmental systems (Genga et al., 2014). The majority of cellulose is extensively used as the raw material for the production of paper and cardboard products. Annually, more than 400 million tons of waste paper are generated (Neelamegam et al., 2018), so waste paper is considered as one of the major components of municipal and industrial solid wastes. As reported, recycling of one ton of waste paper can save 17 trees and 7000 gallons of water, which has great environmental and economic benefits (Lei et al., 2018). However, despite recycling efforts, paper can just be recycled for 2.4 times, and only about 50-65% of waste paper can be useful in creating a new sheet of paper or cardboard box due to the shortening of fiber length and the reduction in tensile strength (Annamalai, Sivakumar & Oleskowicz-Popiel, 2018). A significant amount of waste paper ends up in landfill or incineration, which is a loss of valuable cellulosic raw material and may have negative impacts on the environment. Therefore, expanding the application and techniques, which can convert waste paper into value-added products such as cellulose-based packaging materials, is beneficial to the recycling of waste paper. Recently, a number of attempts have been made on utilization of waste paper and paper-derived materials. The production of biofuels and other sugar derivatives (such as gluconic acid, lactic acid, etc.) from waste paper through biochemical conversion has been reported (Annamalai et al., 2020). The advantage in global production of bioethanol from waste paper is that an estimate of 82.9 billion liters of bioethanol can be produce annually, replacing 5.36% of petroleum consumption, and saving between 29.2% and 86.1% of greenhouse gas (GHG) emissions (Zhang et al., 2015). However, one disadvantage of biochemical conversion, which generally involves enzymatic hydrolysis, is the low enzymatic degradation rate due to the resistant crystalline structure of cellulose and the physical barrier formed by lignin (Zhang et al., 2015). Other potential applications can be cyanoethyl and carboxymethyl cellulose synthesis (Joshi et al., 2015), cellulose nanocrystal production (Orue et al., 2017), heavy metal ion adsorption (Li et al., 2018), and cleaning of spilled oil from water (Li et al., 2017).

Cellulose is a linear homopolymer consisting of D-anhydroglucopyranose units (AGU) linked by β-(1–4) glycosidic bonds, so it is very difficult to dissolve cellulose in common solvents (i.e. water, ethanol and other organic solvents) due to the strong interactions among cellulose molecules (Medronho & Lindman, 2015; Bajpai, 2017). Regenerated cellulose fibers, films, and nonwoven fabrics could be produced through the traditional viscose route. However, this solvent system is technologically complex and requires additional facilities to treat the gaseous and aqueous waste emissions (end-of-pipe technology) (Olsson & Westman, 2013). In recent years, many efforts have been made in developing new solvent systems to dissolve cellulose (Huang et al., 2016; Liu et al., 2017; Minnick et al., 2016; Nishiwaki-Akine et al., 2017; Wei et al., 2017; X. Chen et al., 2018; Z. Jiang et al., 2017). Among them, a novel NaOH/urea aqueous solvent system has been discovered, which can efficiently dissolve cotton linters at low temperature (-12.6 $_{o}$C) in 2 min (Cai & Zhang, 2005). The solubility of wood cellulose in NaOH/urea aqueous solution was studied, and it was demonstrated that wood cellulose could be partially dissolved and form hydrogels due to its high molecular weight (Gong et al., 2014). Recently, it was found that spruce cellulose could be rapidly dissolved in H_2SO_4 aqueous solution at low temperature (Huang et al., 2016). This solvent could directly transfer cellulose with high molecular weight into transparent films without any pre-treatments (Huang et al., 2016). Both these solvents are relatively less energy intensive, and could dissolve cellulose rapidly (in several minutes) in an aqueous environment without using any expensive or toxic chemicals, so they are considered as “green” solvents of cellulose. Therefore, it will be of great interest to investigate the solubility of waste paper and convert it into value-added biodegradable functional materials through these ‘green’ aqueous solvents. To our best knowledge, this attempt has seldom been reported.

1.2 Research Objectives

The overall objective of the present project was to convert waste paper into biodegradable functional materials through an eco-friendly way. In addition to studying the dissolution and regeneration of waste paper in “green” aqueous solvents, this research proposes an investigation in the structure change of cellulose and the relationship between structure and properties of cellulose films and hydrogels. Zinc oxide and essential oil, which have a well-recognized antibacterial and antifungal activity, were used as model chemicals to provide the cellulose films with antimicrobial property.

The specific objectives of this research are:

(1) To evaluate the solubility of waste paper in NaOH/urea and H_2SO_4 aqueous solvents.

(2) To optimize the fabrication of regenerated cellulose films and hydrogels.

(3) To develop cellulose-based packaging films with antimicrobial property.

(4) To develop cellulose hydrogels for controlled release of fertilizer and retention of water in soil.

Chapter 2. Literature Review: Recent development of cellulose materials regenerated from different solvent systems for food applications

2.1 Abstract

Cellulose is the most abundant biopolymer in nature. Cellulose is renewable, biocompatible, biodegradable, and non-toxic. However, strong inter- and intra-molecular hydrogen bonds as well as hydrophobic interactions exist among cellulose molecules. Consequently, it is rendered insoluble in most commonly used inorganic/organic solvents. The traditional cellulose solvent from the viscose process causes serious environmental pollution, so many efforts have been made to develop novel cellulose solvents and study their dissolution mechanisms. Several solvent systems for the direct dissolution of cellulose have been reported, in recent years, which can be classified as acidic aqueous systems, alkali/urea aqueous systems, ionic liquid systems, and mixed solvent systems. Various cellulose-based functional materials, such as films, hydrogels, and aerogels, can be regenerated from these solvent systems, and have attracted more and more attention. The purpose of this literature review is to summarize the recent development of cellulose-based materials with potential applications in food related fields, including food packaging, food thermal insulation, encapsulation of micronutrients and nutraceuticals, water treatments, and food agriculture.

2.2 Introduction

Cellulose is a linear carbohydrate polymer that is the most abundant in nature (Yohana, Sriwidodo, & Abdassah, 2019). Its reported sources vary and can be classified into two groups: 1) wooden sources and 2) non-woody lignocellulosic materials (Yohana et al., 2019). For wooden sources, hardwoods (i.e. deciduous broadleaf) and softwoods (i.e. evergreen conifers) are the major sources (Landín et al., 1993; Thoorens et al., 2014). As for non-woody lignocellulosic materials, there are cotton materials, such as cotton linters, cotton fabric waste and cotton stalks, and the other plant sources, such as soybean husk, sugarcane bagasse, corn husk and oil palm empty fruit bunch (Ahmad et al., 2018; El-Sakhawy & Hassan, 2007; Han et al., 2015; Nakasone, Ikematsu, & Kobayashi, 2016; Uesu, Pineda, & Hechenleitner, 2000; J. Zhang et al., 2017; Zhang et al., 2016). The interest in developing cellulose based materials for value-added applications has been gaining attention, as cellulose is a renewable natural resource that is readily available, biodegradable, biocompatible and non-toxic (Sadeghifar et al., 2017).

In terms of structure, cellulose is a homopolysaccharide chemically composed of D-glucose repeating units (or anhydroglucopyranose unit (AGU)) that are linked together by β 1-4 glycosidic bonds (Medronho & Lindman, 2015). In addition, cellulose has a degree of polymerization (DP) that varies and is dependent on the type of source; thus, DP can be from 100 to 2000 or to a higher extent 10,000 to 15,000 (Bajpai, 2017; Medronho & Lindman, 2015). Cellulose, in nature, is a semi-crystalline structure composed of high crystalline domains and low amorphous regions (Klemm et al., 1998). Several polymorphs of crystalline cellulose exist: Cellulose I is the natural structure; Cellulose II is regenerated through solubilization and recrystallization; Cellulose III can be made from Cellulose I or II via liquid ammonia treatments; and Cellulose IV is formed through thermal treatments (Bajpai, 2017). Moreover, cellulose is held together by a network of intra- and intermolecular hydrogen bonds (Medronho & Lindman, 2015). In addition, cellulose is amphiphilic in nature, which has hydrophilic hydroxyl groups (-OH) on the equatorial portion of the ends of AGU chains and hydrophobic C-H bonds on the axial portion of the ends of AGU chains (Medronho & Lindman, 2014; Medronho et al., 2012). The chemical structure of cellulose can be visually represented below in the diagram 2.1 (Kallos & Apostolopoulou, 2020).

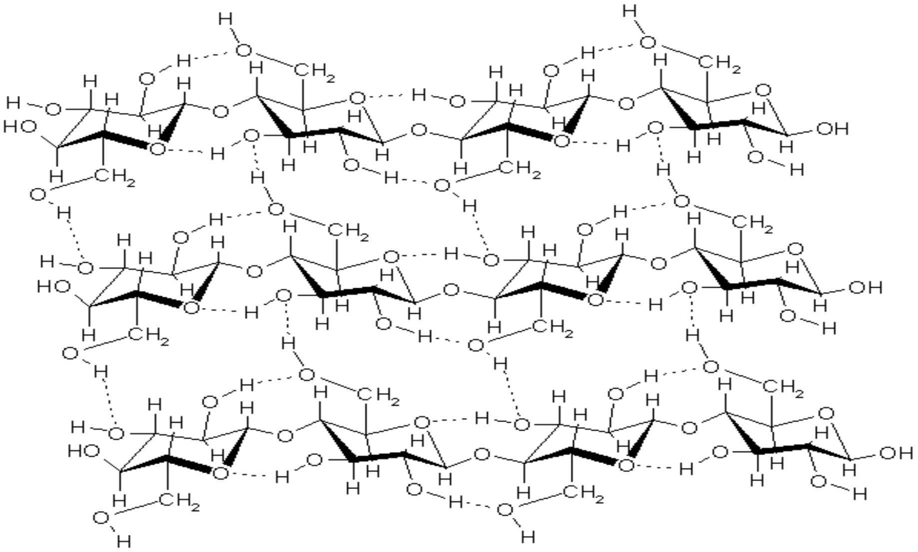

Fig. 2.1 Cellulose molecular structure (Kallos & Apostolopoulou, 2020)

Due to the linear structure and strong interactions, the dissolution of cellulose in common inorganic/organic solvents, such as water, ethanol and other organic solvents is a challenge. At the same time, cellulose is not a thermoplastic and will degrade during high temperature treatments (Bajpai, 2017). Thus, a suitable solvent that is low cost and eco-friendly is required to dissolve and regenerate cellulose into various value added materials. Several solvent systems of cellulose have been reported in recent years, which can be classified as acidic aqueous systems, alkali/urea aqueous systems, ionic liquid systems, and mixed solvent systems (Chen et al., 2018; Huang et al., 2016; Jiang et al., 2017; Jiang et al., 2014; Liu et al. 2017; Minnick et al., 2016; Nishiwaki-Akine et al., 2017; Sundberg et al., 2015; Wei et al., 2017). Based on these solvent systems, different regenerated cellulose materials such as films, hydrogels, and aerogels, have been developed for the applications in food, agriculture, medicine, environment, and electronic devices. This literature review focuses on the recently reported cellulose based functional materials for food related applications. The mechanism of dissolution and regeneration of cellulose in different solvent systems is also summarized.

2.3 Different Cellulose Solvent Systems and Their Dissolution Mechanisms

A traditional and well-known way that cellulose has been dissolved and processed is called the viscose process (Olsson & Westman, 2013). This process involves a reaction of converting cellulose into a derivative form (cellulose xanthogenate, or xanthate) with carbon disulfide. The resultant cellulose xanthate is soluble in aqueous sodium hydroxide and the viscous liquid can be then regenerated into viscose textiles and cellophane functional materials through acid precipitation (Olsson & Westman, 2013; Sjostrom 1993). Although this method is successful and has been used for many years, it has presented drawbacks from an environmental point of view, because many sulfuric reagents and their by-products and heavy metals result as residues, from this process, which can pollute the air and water streams. Therefore, the disposal of the used solvents has been a challenge (Olsson & Westman, 2013), and the development of novel alternative solvents that can directly dissolve cellulose in a cost effective and non-toxic way is necessary. Thus, novel alternative solvents were further classified and their dissolution mechanism was discussed in this following section.

2.3.1 Acidic Aqueous Systems

Concentrated acid solutions (above 50 %) are usually used for the hydrolysis of cellulose (Freudenberg, 1936). However, Huang et al. recently reported that spruce cellulose with a relatively high molecular weight (4.10×10^5g mol^{-1}) can rapidly dissolve in concentrated (64 wt%) sulfuric acid (H_2SO_4) at low temperatures (-20^{o}C) (Huang et al., 2016). The dissolution of cellulose in sulfuric acid aqueous solutions with different acid concentrations was observed by using optical microscope, and the spruce cellulose fibers gradually faded and completely disappeared after 5 min in 64 wt% H_2SO_4 solution. The structure change of cellulose during dissolution and regeneration was characterized by FT-IR and XRD, and the dissolution mechanism was proposed, that the protons (H^+) and the sulfate (SO_4^{2-}) anions could readily penetrate into the crystalline and amorphous regions of spruce cellulose and “switch-off” the strong hydrogen bonds by attaching to the hydroxyl groups of cellulose. No new peaks appeared in FTIR results of regenerated cellulose, confirming that direct physical dissolution took place rather than formation of cellulose derivatives. At the same time, a transition from cellulose I to cellulose II occurred, indicating that spruce cellulose was dissolved rather than being hydrolyzed by concentrated sulfuric acid. The molecular weight of spruce cellulose decreased during dissolution, but the degradation was relatively slow, and the final molecular weight of cellulose was still larger than the sample from other plant sources such as cotton linter pulp (Huang et al., 2016).

Another acid aqueous solvent system has been reported by Nishiwaki-Akine et al. (Nishiwaki-Akine et al., 2017). It was observed that Japanese beech wood cellulose could be dissolved in pure formic acid in 4 to 7 days at room temperature. The dissolution process was monitored by characterizing the transparency of cellulose/formic acid suspension, which increased linearly with dissolution time and the color became darker (brown). The viscosity of solution increased, as well, until 7 days; however after 7 days, a decrease in viscosity was observed which was probably caused by the hydrolysis of wood cellulose in formic acid. Therefore, the dissolution of wood cellulose in formic acid solution occurred as a result of mild hydrolysis. The process took a longer time since formic acid is weaker than H_2SO_4 (Nishiwaki-Akine et al., 2017).

2.3.2 Alkali/Urea Aqueous Systems

A novel solvent of cellulose, namely 7 wt % NaOH/12 wt % urea aqueous solution pre-cooled to -12 $_{o}$C, was initially developed by Zhang's group (Cai & Zhang, 2005; Cai et al., 2008). It represents the most rapid dissolution of native cellulose, and cellulose with weight-average molecular weight (M_w) lower than 1.2×10^5 g mol^{-1} could be dissolved in NaOH/urea aqueous solution within 2 min (Cai & Zhang, 2006). It has been demonstrated that the rapid dissolution of cellulose could also occur in 4.6wt% LiOH/15wt% urea and 5wt% NaOH/4.5wt% thiourea aqueous solution at -12 ºC and -5 ºC within 2 min, respectively (Lue, Zhang & Ruan, 2007; Cai et al., 2007). The dissolution mechanism further emphasized that the low-temperature played an important role in creating an inclusion complex (IC) structure through hydrogen bond networks between cellulose and solvent molecules, leading to the dissolution of cellulose macromolecules in the aqueous solution (Lue & Zhang, 2008). The IC hosted by thiourea and NaOH, in which cellulose chain attached to NaOH hydrates, could aggregate to form a sphere having mean size of 60 ~ 160 nm. The NaOH or LiOH hydrates could cleave the chain packing of cellulose through the formation of new hydrogen bonds at low temperatures, resulting in a relatively stable complex associated with LiOH, water clusters and cellulose. A channel IC hosted by urea encaged the cellulose macromolecule in LiOH/urea solution with prior cooling, and could provide a rationale on forming a good dispersion of cellulose (Lue & Zhang, 2008). This solvent system has been widely applied and further developed in recent years. Jiang et al. reported the dissolution mechanism of microcrystalline cellulose in NaOH/urea aqueous solution at -12$_{o}$C (Jiang et al., 2014). The NMR results confirmed that direct intermolecular hydrogen bonds formed between the hydroxyl (OH^-) anions of NaOH and water (H_2O) and the amino groups of urea, but urea did not interact with cellulose. The Na^+ cations from NaOH directly interacted with both cellulose and urea, which led to the formation of inclusion complexes comprised of cellulose-NaOH-urea-H_2O (as shown in Fig. 2.2). The urea-OH^- clusters played a crucial role in enhancing the stability of Na^+ cation attraction to cellulose, and the low temperature allowed the stable hydrogen interactions in urea-OH^- clusters. The formation of cellulose-NaOH-urea-H_2O inclusion complexes was confirmed by TEM observation as an extended conformation with a mean diameter of 3.6nm and a mean length of about 300nm (Jiang et al., 2014).

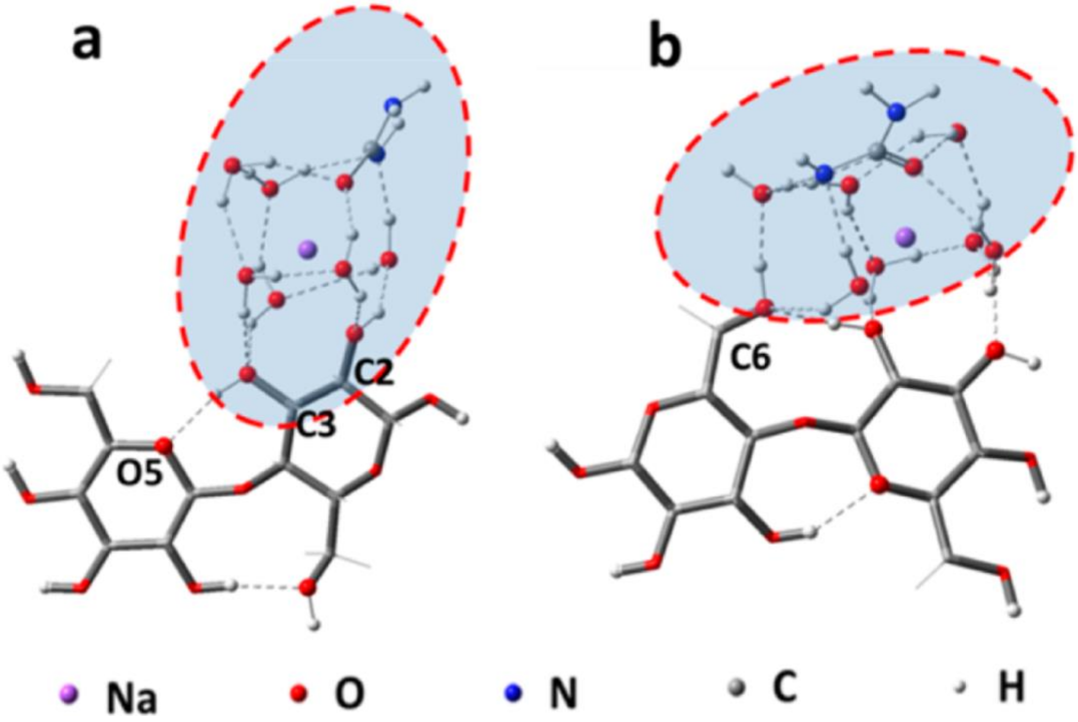

Fig. 2.2 Optimized structures of (a) Cell-Cluster-O2,3 and (b) Cell- Cluster-O6 by the M06-2X/6-31+G(d) theoretical method (Jiang et al., 2014).

The NaOH/thiourea aqueous system has also been further studied, and an optimal condition of 9.3wt% NaOH/7.4wt% thiourea was determined to dissolve cotton linter pulp at 8°C within 5 min

(Jiang et al., 2017). A difference in temperature could be emphasized to indicate that a higher temperature of 8^{o}C rather than -12^{o}C was used to dissolve cellulose, because thiourea formed metastable OH complexes with cellulose in solution. This improved temperature condition could save energy during dissolution and promote the application of this solvent system (Jiang et al., 2017).

A novel alkali/urea system, in which tetra-butyl-ammonium hydroxide (TBAH) was employed as a bulky base, was used to dissolve microcrystalline cellulose under ambient conditions (Wei et al., 2017). It was found that the dissolution mechanism of cellulose in this solvent was quite different from the former ones. The result of differential scanning calorimetry (DSC) test revealed that TBAH in aqueous solution has an amphiphilic property and it could be flexibly adjusted for dissolving cellulose in the optimal concentration range of 40 to 60 wt%. The role of urea was determined via ^{13}C-NMR measurements, where urea served as a dissolution promoter of cellulose. When the concentration of urea in TBAH aqueous solution was higher than 0.2:1 (w/v), cellulose could completely dissolve as a transparent solution under ambient conditions. As shown in Fig. 2.3, upon dissolution, TBAH formed hydrate ions and combined with urea as a hybrid complex solvent. This hybrid complex solvent was regarded as a hydrophobic contributor where its amphiphilicity could be adjusted. Consequently, when cellulose was added to this hybrid complex solvent, if the solvent was adjusted to the suitable amphiphilicity that matched the surface property of cellulose, the solvent molecules could infiltrate into cellulose fibers and decrease the interfacial resistance between the surface of cellulose crystal and the solvent. Then, water molecules could penetrate into the crystal structure and destroy the hydrogen bonds among cellulose molecules, resulting in the dissolution of cellulose (Wei et al., 2017).

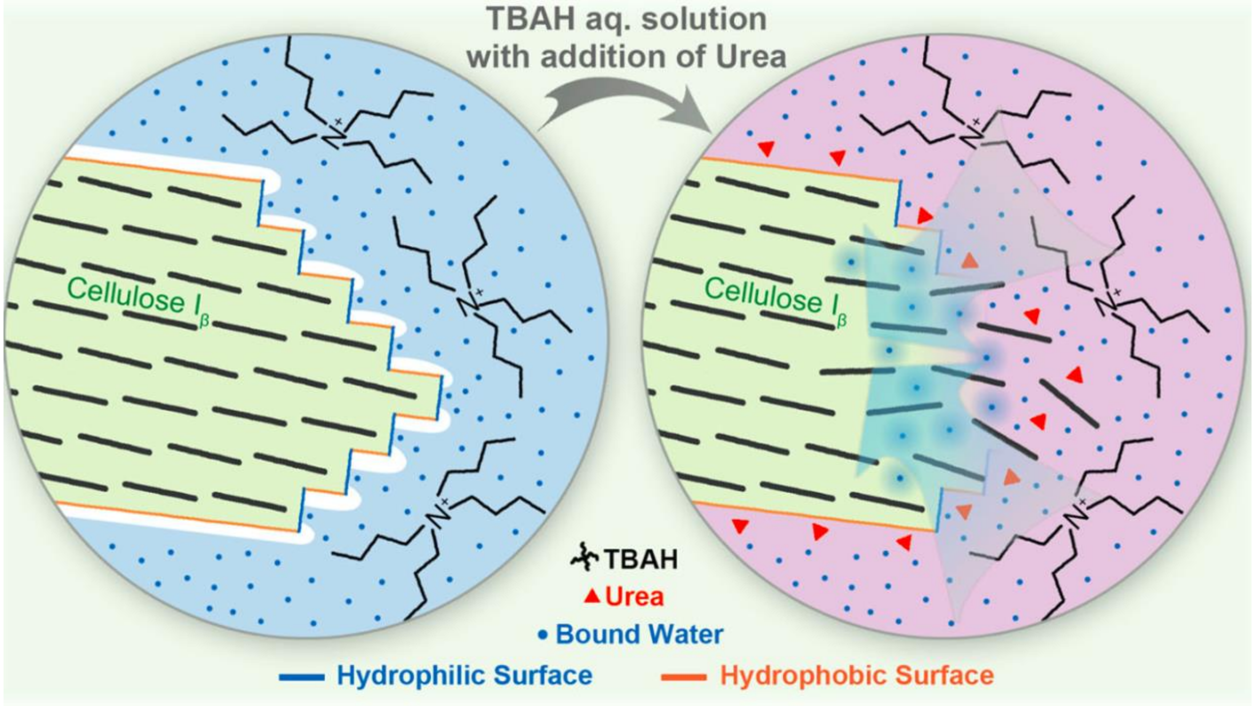

Fig. 2.3 Schematic representation of the mechanism for dissolution of cellulose in TBAH/urea aqueous solution. These two diagrams show different interfacial resistances between the crystal surface of natural cellulose and the solvent in the dissolution of cellulose in a "hydrophilic solvent and an amphiphilic solvent", respectively (Wei et al., 2017).

2.3.3 Ionic Liquids (ILS)

An ionic liquid is a salt composed of an organic cation and an organic/inorganic anion with low melting point (below 100$_{o}$C). From the late 1990s up until now, ionic liquids have been used in various areas, such as pharmaceutics, analytical chemistry, separation and extractions, material science and electrolytes in batteries (Olsson & Westman, 2013). Ionic liquids have also been studied for cellulose dissolution, as they are powerful non-derivatizing solvents of cellulose, which are non-volatile and can aggressively break hydrogen bonds of cellulose (Liu et al., 2017). Liu et al. recently reported the dissolution of cellulose nanocrystals extracted from bleached wood pulp in 1-allyl-3-methylimidazolium chloride (AmimCl) ionic liquid (Liu et al., 2017). It was found that, during the dissolution, the allyimidazolium cations (Amim$_{+}$) from the ionic liquid were able to interact with the negatively charged sulfate half-ester groups of cellulose and the Cl$_{-}$ anions from the ionic liquid interacted with the hydroxyl protons of cellulose (Liu et al., 2017). Sundberg et al successfully dissolved spruce cellulose in ethy1-3-methylimidazolium acetate (EmimAc) ionic liquid at 70$_{o}$C (Sundberg et al., 2015). Similar to AmimCl, EmimAc is represented by the cation (Emim$_{+}$) and the anion (Ac = CH_3COO_{-}). The dissolution process was studied by monitoring the change in rheological properties of cellulose/EmimAc solution. The solution exhibited a shear-thinning behavior at both 25 and 70 $_{o}$C due to the alignment of cellulose molecular chains; however, the viscosity was lower at 70 $_{o}$C than that at 25 $_{o}$C, and it took much less time for dissolution at 70 $_{o}$C (Sundberg et al., 2015).

2.3.4 Mixed Solvent Systems

2.3.4.1 Alkali and co-solvent system

Co-solvents are supplementary solvents with negligible capacity, on their own, but when added to solvent systems, they can increase the dissolution efficiency of cellulose by reducing dissolution time, temperature and solution viscosity. Examples of these co-solvents are polar aprotic solvents, such as dimethyl-sulfoxide (DMSO), dimethylformamide (DMF) and 1,3-dimethyl-2-imidazolidinone (DMI) (Minnick et al., 2016). Chen et al reported that microcrystalline cellulose (MCC) with a concentration of 9.19% was successfully dissolved in 20wt% TBAH/80wt% dimethyl-sulfoxide (DMSO) co-solvent system at room temperature within 5 min (Chen et al., 2018). It was explained that, DMSO radicals formed in TBAH/DMSO mixed solvent could attack the reducing AGU terminals of MCC and cause the destruction of MCC structure. Consequently, the intermolecular hydrogen bonded network of MCC was exposed to the TBAH/DMSO mixed solvent to cooperatively dissolve MCC. During this process (as shown in Fig. 2.4), the amount of DMSO radicals was positively correlated with the dissolution of MCC, so the dissolution was accelerated as the content of DMSO in the mixed solvent system increased (Chen et al., 2018).

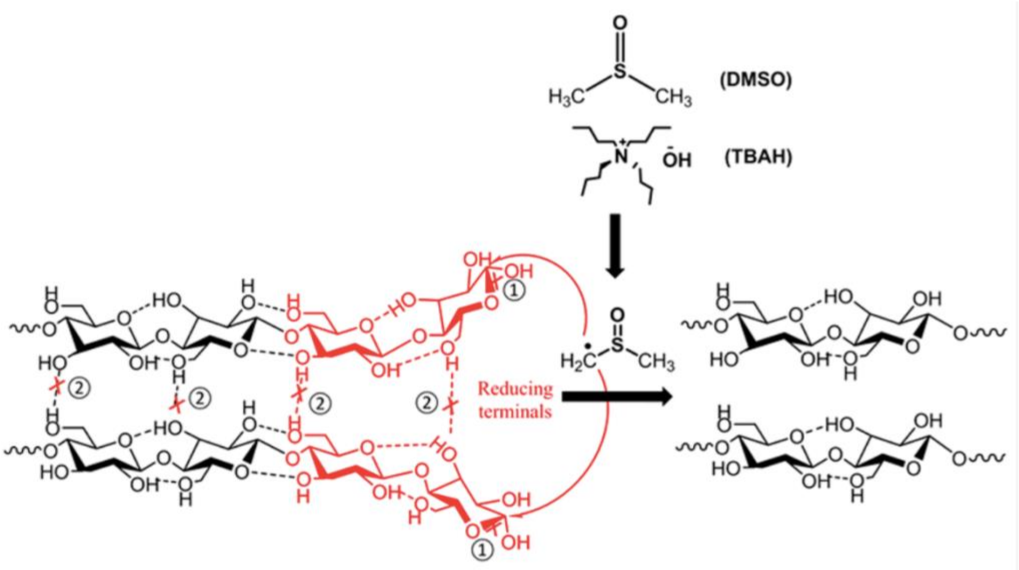

Fig. 2.4 Proposed graphic cellulose dissolution mechanism: 1) represents the radical attack at the reducing terminals; 2) represents the opening up of MCC chains from the reducing terminals and destruction of the intermolecular hydrogen bonds (Chen et al., 2018).

2.3.4.2 Ionic liquid, anti-solvent and co-solvent systems

Contrary to co-solvents, antisolvents are solvents used to separate or precipitate solutes in solution. In the context of cellulose dissolution in ILs, all aqueous and inorganic/organic solvents (i.e. water, alcohols etc.) can precipitate cellulose from ILs. Those antisolvents are usually protic solvents and have hydrogen bond donating properties that can compete with ionic liquid anions, which can interfere with the IL's ability to dissolve cellulose (Minnick et al., 2016). The dissolution of MCC in IL/anti-solvent systems and IL/co-solvent systems has also been studied (Minnick et al., 2016). Minnick et al chose the ionic liquids (1-ethyl-3-methylimidazolium phosphate ([Emim][DEP]) and 1-butyl-3-methylimidazolium ([Bmim][Cl])), aprotic co-solvents (DMSO, dimethylformamide (DMF) and 1,3-dimethyl-2-imidazoliddinone (DMI)), and protic anti-solvents (water, methanol and ethanol) as models to evaluate the effects of different mixed solvent systems and temperatures (40-120$_{o}$C) for the dissolution of MCC. It was revealed that MCC could be dissolved directly at a maximum concentration of approximately 20 wt% at temperatures above 100$_{o}$C. The anti-solvents significantly reduced the solubility of MCC by 38-100%, while the aprotic co-solvent mixtures up to 1:1 ratios enhanced the dissolution of cellulose by 20-60% (as shown in Fig. 2.5). Through Kamelet-Taft (KT) solvatochromic analysis, FT-IR and NMR, it was confirmed that the dissolution of cellulose in IL-mixed solvents was based on the increased basicity and decreased acidity of the solvent paired with IL. All the co-solvents mixed with IL [Emim][DEP] had moderate hydrogen bonding and low hydrogen bond donating abilities.

Thus, the co-solvents did not compete with the IL's anions to interact with the hydroxyl groups of cellulose. Instead, the co-solvents could interact with IL ions and break their ionic clusters, which thereby regenerated ion pairs and free anions to interact with the cellulose molecules. This was why the dissolution of cellulose was enhanced with the presence of co-solvents. On the other hand, [Emim][DEP]-anti-solvent systems gave the opposite effects, where the basicity decreased and the acidity increased. The solubility of cellulose reduced because IL interacted more with the anti-solvents (Minnick et al., 2016).

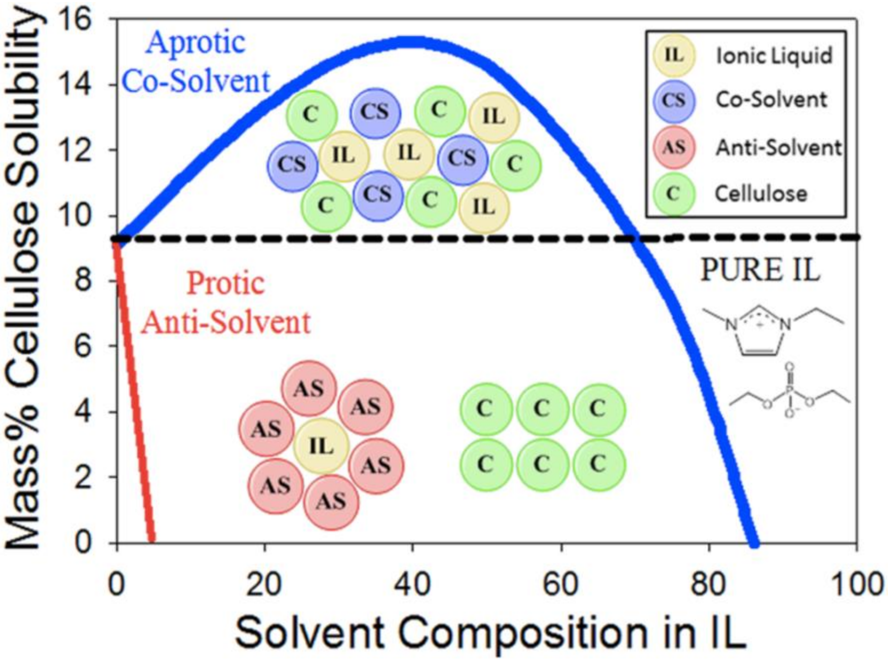

Fig. 2.5 Cellulose Dissolution in Ionic liquid/Anti-solvent and Co-solvent System (Minnick et al., 2016)

2.4 Food Related Applications of Regenerated Cellulose (RC)

Over recent years, there has been a rising interest in regenerated cellulose materials, as they are renewable, biodegradable, biocompatible and non-toxic. In turn, because of these properties, they can be developed as value-added commodities and applied in different areas, such as food, agriculture, medicine, environment, and electronic devices. Especially, food related applications have attracted more and more attention, which could be summarized in the following areas: food packaging, food thermal insulating materials, encapsulation of nutraceuticals and micronutrients, water treatments and food agriculture.

2.4.1 Food Packaging

Regenerated cellulose films are usually transparent and have a certain level of mechanical strength and gas barrier property, so they can be directly used as biodegradable packaging materials. Nishiwaki-Akine et al. reported that transparent cellulose films could be regenerated by direct dissolution of fine Japenese beech wood in formic acidic at room temperature within 4 to 7 days (Nishiwaki-Akine et al., 2017). The films were regenerated by simply slow evaporation of the solvent, and were very bendable and foldable with a relatively high tensile strength and Young's modulus. They also showed good thermal stability, and could be used at up to 180$_{o}$C without softening. These wood cellulose films prepared through a very simple method were highly sustainable and biodegradable, and have potential applications as packaging materials (Nishiwaki-Akine et al., 2017).

The regenerated cellulose materials are also a promising matrix for the fabrication of functional composites. Various organic/inorganic compounds could be mixed in cellulose solutions and then incorporated in the regenerated cellulose matrix to endow the material with functional properties. Wang et al. reported that cotton linter pulp was dissolved in lithium hydroxide/urea solvent, and then different amounts of attapulgite (ATT, 5 to 20 wt%) were added to prepare RC/ATT composite films (Wang et al., 2018). ATT is a clay composed of hydrated magnesium aluminum silicate mineral, and was dispersed in cellulose film matrix with a homogeneous distribution. The addition of ATT improved the mechanical properties of RC films. When the content of ATT was 5 wt%, the tensile strength and Young's modulus of RC film increased from 86.9MPa and 4.3GPa to 127MPa and 5GPa, respectively. The incorporation of ATT in RC films also enhanced the thermal stability and reduced the water absorption. Especially, low oxygen permeability of below 0.5 cm$_3$ μm/day m$_2$ kPa was achieved in RC/5wt%ATT film, which could be even lower with 20wt% ATT in RC film (0.32 cm$_3$ μm/day m$_2$ kPa). However, ATT affected the optical property of RC film. When the content of ATT was 20 wt%, the transparency decreased from 85.5 % to 0.7% (Wang et al., 2018). It might not be desirable when the transparency is an asset.

ZnO-cellulose nanocomposite (ZNC) films were regenerated from cellulose-NaOH/urea/zincate solution, which was prepared based on the bioinspired mineralization (Fu et al., 2017). Dissolution of cellulose occurred because non-acid coagulants (NaOH, urea and zincate) formed an inclusion complex with cellulose. This further allowed for the mineralization of ZnO nanoparticles in the regenerated cellulose films at room temperature. These ZnO nanoparticles had good interfacial interaction with cellulose, and the composites showed good mechanical properties (tensile strength: 46.7 MPa, and elongation at break: 6.4%). The appearance of ZnO nanoparticles endowed the regenerated cellulose films with good antimicrobial activity against *S. aureus* and *E. coli bacteria*. Varied ranges of inhibition zones were observed for S. aureus (2.8-4.4 mm) and E. coli (3.3-4.7 mm). The ZnO/cellulose composite films also exhibited excellent photocatalytic properties. The degradation efficiency of rhodamine B reached to 99.3% under UV light after 50 min, and only a slight decrease was observed after 3 cycles. Therefore, these composites could be applied not only in active food packaging, but also in eliminating organic pollutants in wastewater (Fu et al., 2017).

Microcrystalline cellulose was dissolved in an ionic liquid/co-solvent medium (1-ethyl-3-methylimidazolium acetate and 1-butyl-3-methylimidazolium acetate / dimethyl sulfoxide (DMSO)) at room temperature, and the cellulose solution was doped with titania (TiO_2) and magnetite (Fe_2O_3) nanoparticles to prepare photocatalytic and magnetic porous films (Wittmar et al., 2017). TiO_2 is an inorganic material that can be utilized for a broad range of applications, such as corrosion protection, optical coatings, gas-sensors, solar cells and photo-catalysis, while Fe_2O_3 has super magnetic properties and good biocompatibility. The cellulose based nanocomposites were fabricated via non-solvent induced phase separation and thus had multi-functions. For example, their photocatalytic property could be involved in water purification and self-cleaning material. When induced with a high frequency alternating magnetic field (AMF), the incorporated Fe_2O_3 nanoparticles could act as nano-heaters to trigger temperature-sensitive response for controlled release (Wittmar et al., 2017).

Cellulose is not a thermoplastic, but it can be mixed with the other natural or synthetic polymers including thermoplastics. Zhang et al. developed a simple method via dissolution, gelation, isolation and melt extrusion to make RC/poly(ethylene oxide) (PEO) composite films (Zhang et al., 2016). Cellulose from cotton linter was dissolved in NaOH/urea aqueous solution, and then casted and regenerated in distilled water into a hydrogel. The addition of PEO isolated the cellulose in the hydrogel, and the final melt extrusion provided a shear force to breakdown the cellulose hydrogel network into small particles so as to be dispersed in PEO matrix. It was observed from SEM and TEM that an ordered dispersion of cellulose nanoaggregates (size: 50-100nm) and quasi-nanospheres (size: 10-30nm) existed in RC/PEO composite films, leading to the greatly enhanced tensile strength and Young’s modulus by 146% and 276%, respectively, when compared to pure PEO film. It was worth noting that the resultant composite materials were biodegradable and mouldable at a certain elevated temperature (Zhang et al., 2016).

2.4.2 Food Thermal Insulating Materials

Insulating materials usually have porous aerated structures with low thermal conductivity (Cuce, E., Cuce, P., Wood, & Riffat, 2014). Cellulose aerogels have been considered as a promising insulating materials, as they have abundant pores in their internal structure that allow for good heat insulating performance (Han et al., 2015). However, it is easy to ignite cellulose; thus, the addition of flame retardant in cellulose aerogels is necessary for the applications at high temperature (Han et al., 2015). Han et al. reported that cellulose from waste cotton fabrics (WCFs) could be utilized to make flame retardant and heat insulating aerogels (Han et al., 2015). WCFs cellulose was dissolved in NaOH/urea aqueous solvent and regenerated in 5 wt% H_2SO_4 aqueous solution. The regenerated cellulose hydrogels were washed in deionized water and immersed in magnesium chloride solution, and then dipped in NaOH to synthesize the magnesium hydroxide nanoparticles (MH NPs) in the hydrogels. Finally, MH NPs hydrogels were converted into MH NPs aerogels by removal of water via lyophilization. It was revealed that, cellulose aerogels served as a three-dimensional nano-porous scaffold for the non-agglomerated growth of MH NPs. MH NPs aerogels showed excellent flame retardancy, which could be extinguished within 40 s. The existence of MH NPs didn't affect the heat insulating performance, which only moderately increased from 0.056 to 0.081 $Wm^{-1}k^{-1}$. Thus, MH NPs aerogels were a novel biodegradable insulation material that could be used to replace synthetic polystyrene as the packaging material to retain desired temperatures of chilled or hot food and beverages (Han et al., 2015; Mikkonen et al., 2013).

2.4.3 Encapsulation of Micronutrients and Nutraceuticals

Encapsulation is the process by which a membrane is created around a substance to provide a protective barrier from the surrounding environment (Cook et al., 2012). Many micronutrients and nutraceuticals supplements have health promoting effects; however, they are sensitive to processing and storage environments, such as change in temperature, pH and types of fluids they are exposed to, and their psychochemical properties can change if they are not protected. Thus, encapsulation technology has been used to protect and deliver micronutrients and nutraceuticals to their targeted sites (Luan et al., 2018). Important requirements for encapsulation wall materials are their capacities of loading and controlled-releasing the substances and their resistance to environments. For example, the encapsulating materials with pH-responsive properties could survive in harsh acidic gastric fluid environments, and release the substances at the correct pH in the intestine (Saito et al., 2007).

Cellulose based three-dimensional porous structures have been employed as promising encapsulating delivery vehicles of nutraceuticals. Luan et al. fabricated cellulose macrogels comprised of cellulose fibers/cellulose nanofibers (CCNMs) as a vehicle to release probiotics in intestine (Luan et al., 2018). Cellulose nanofibers (CNFs) were prepared via TEMPO-mediated oxidation and contained carboxyl groups on fiber surface. They served as pore size regulator through pH-stimulated response for the loading and controlled release of probiotics. CCNMs were prepared by dissolving cellulose fibers in LiOH/urea aqueous solvent at -20 $_{o}$C and mixed with CNFs. The composite solution was dropwise extruded from a syringe into dilute hydrochloric acid (10%) coagulation bath to form macrogels, which were then washed and freeze-dried. The CCNMs samples were loaded with L. *plantarum* strain probiotics, and the release behavior of probiotics in simulated gastric fluid (SGF) and simulated intestinal fluid (SIF) was studied. The obtained macrogels had a porosity of 92.68% and the content of CNFs was 90%. This highly porous structure benefited the infiltration of probiotics, and the high content of CNFs in macrogels allowed the release of probiotic of up to 2.68x10 ^{8}Cfu/ml in the targeted intestinal tract region (Luan et al., 2018).

Microcrystalline cellulose (MCC) derived from cotton linter was dissolved in ionic liquid/co-solvent medium (1-butyl-3-methylimidazolium [BMIM][Cl]/DMF) and regenerated into spongy cellulose particles/beads that could encapsulate hydrophobic and hydrophilic non-volatile solutes (Omura et al., 2017). These cellulose particles/beads had a spongy structure, which could be retained upon wetting in different media. They could then encapsulate the non-volatile solutes regardless of the hydrophobic/hydrophilic nature, and the encapsulation efficiency exceeded 80%. Rhodamine B and Nile Red were selected as the model solutes, and their release could be further controlled via the addition of conventional polymer poly(methyl methacrylate) (PMMA), which was applied by dipping cellulose beads in a PMMA/chloroform solution (Omura et al., 2017).

Lightweight, highly compressive non-crystalline gas-filled cellulose gel capsule was regenerated from non-modified cellulose-rich wood fiber solution (Carrick et al., 2014). The raw material was initially dissolved in LiCl/N,N-Dimethylacetamide (DMAc) solvent system, and then the solution was saturated with soluble propane gas, and was added dropwise into non-solvents (water, methanol and propanol) to prepare cellulose gel capsules with propane gas bubble inside. The cellulose capsules had a diameter of 3mm, a wall thickness ranging from 4 to 8 μm, and a density of 7-14 kg/m^3. The properties of cellulose capsules could be modulated depending on the solubility of propane gas in the selected non-solvents for regeneration. The dry cellulose capsules had a remarkable compressive recovery due to the encapsulated propane gas that enhanced the mechanical integrity. These capsules were potential load-carriers of micronutrients for supplementation of important vitamins and minerals (Carrick et al., 2014).

2.4.4 Water Treatments

Decontamination of water from various impurities, such as heavy metal ions, organic pollutants, pharmaceuticals, dyes from consumer products and waterborne pathogens is a need, as rapid urbanization and expanding industrial activities increase demands for cleaner drinking and wash water for the sake of public health (Li et al., 2018; Zhao et al., 2017; Kim et al., 2014). Composite adsorbents and membranes can be constructed to serve as filters to clean various impurities found in water, and cellulose-based materials are excellent matrices as they are renewable, biocompatible and biodegradable.

Li et al. reported a novel all-cellulose adsorbents for the removal of dyes from waste water (Li et al., 2018). The absorbents were fabricated by dissolving filter paper in NaOH/urea aqueous solution, and the processed micro-fibrillated cellulose (MFC) and nano-$CaCO_3$ were added to the solution as the reinforcing fillers and pore-forming agent, respectively. The mixture was then regenerated in HCl aqueous solution. The carboxyl groups on the surface of MFC and the large surface area enabled the outstanding adsorption capacity. These all-cellulose adsorbents had a maximum adsorption capacity of 303 mg g^{-1} for methylene blue, which was relatively higher than most bio-based adsorbents (Li et al., 2018).

Porous hybrid fibers (PHFs) were fabricated by a novel one-step process (Zhao et al., 2017). Cotton was pre-treated with water, methanol and N,N-dimethylacetamide (DMAc), and dissolved in LiCl/DMAc solvent with the addition of $FeCl_3$. The obtained solution was spun in NaOH aqueous bath and then lyophilized to prepare cellulose/$Fe(OH)_3$ PHFs. It was revealed that PHFs had a multi-scale porous structure, and $Fe(OH)_3$ nanoparticles were uniformly distributed in cellulose fibers. Congo red was selected as a dye model, which could be removed from water by PHFs at a maximum capacity of 689.65 mg/g. These PHFs were also able to favorably remove the dye via filtration adsorption at natural pH with excellent reusability (Zhao et al., 2017).

Kim et al. developed m-aramid/cellulose composite membranes as a water disinfection treatment through non-pressure driven filtration (Kim, Lee, & Jeong, 2014). Cellulose pulp was dissolved in LiCl/DMAc solvent and blended with m-aramid. The composite membranes were obtained by coagulating the cellulose/m-aramid solution in a water bath. The addition of m-aramid endowed the composite membranes with the capacity to disinfect water by removing microorganisms. The water disinfection efficacy from unchlorinated m-aramid/cellulose composite membranes against gram-negative (*E.coli.*) and gram-positive (*S.Aureus*) bacteria was 1-log reduction in their CFU counts, respectively. This efficacy could be further improved to 5-log reduction in their CFU counts by chlorinating the m-aramid/cellulose composite membranes, which could be used as a simple environmental friendly means of disinfecting contaminated water for drinking (Kim et al., 2014).

2.4.5 Food Agriculture

In food agriculture, most crops are aerobic organisms that depend of steady supplies of oxygen from the environment. Consequently, waterlogging is a stress factor to seed plants as it inhibits the oxygen supply to the roots and limits the respiration of the plant. As a solution to this problem, hydrogels have been considered to be an attractive functional material because they are hydrophilic systems that can preserve nutrients and reserve significant amounts of water and then can gradually release them to root systems, so plants can have a steady oxygen environments to grow (Zhang et al., 2017). Cellulose hydrogels are biodegradable and can hold certain amount of water in the three-dimensional network, so they also have potential applications in agriculture. Zhang et al. recently reported the growth of sesame seed in regenerated cellulose hydrogels (Zhang et al., 2017). Softwood sulphite pulp was firstly converted into oxidized nanofibers via TEMPO-mediated reaction, and then dissolved in NaOH/urea aqueous solvent. Cellulose was crosslinked by the chemical reagent epichlorohydrin to form anionic cellulose hydrogels with a microporous structure and excellent water absorption capacity. Seed germination tests showed that the obtained anionic cellulose hydrogels had enough carboxylate groups to promote the growth regulation for seed germination of sesame, while the fungal growth tests indicated an antimicrobial activity. Thus, these anionic cellulose hydrogels could be applied for plant growth in soilless mediums (Zhang et al., 2017).

2.5 Conclusion

In the past five years, there have been numerous studies that focused on the dissolution and regeneration of cellulose from different raw materials. Various solvent systems, namely acidic solutions, alkali/urea aqueous solvents, ionic liquids, and mixed solvent systems, were applied to dissolve cellulose, and their dissolution mechanism was investigated in detail. In acidic systems, the dissolution is governed by two competing reactions, which are the disruption of hydrogen bonding network of cellulose via ionic interactions from the acids and the controlled form of hydrolysis. In alkali/urea systems, two dissolution strategies are presented. The first is the disruption of cellulose hydrogen bonds by more stable and/or metastable hydrogen bonds from solvents that can form clusters of inclusion complexes. The second is based on the amphiphilic character of cellulose, where the semi-crystalline structure can be disrupted by compatibly adjusting solvents, so they can penetrate and dissociate the cellulose structure. In ionic liquid systems, cellulose dissolution strategy is primarily based on disrupting the cellulose hydrogen bonding network via ionic interactions. Finally, in mixed solvent systems, both the amphiphilic character and the disruption of hydrogen bonding network of cellulose are used to effectively dissolve cellulose.

Despite of different solvent systems, cellulose solutions could be regenerated into various forms by replacing with a non-solvent. Cellulose particles, films, and hydrogels with different dimensions could thus be obtained. Their properties could be modified through physical and chemical methods, for example, the addition of inorganic nanoparticles or another polymer to form a composite, the chemical crosslinking to strengthen the network structure, and so on. With these well-designed structures and properties, cellulose-based materials have a wide potential application in many areas, including food science. Current researches mainly focused on the following food related applications: (1) composite and biodegradable films for “smart”, active and environmentally friendly food packaging; (2) aerogel based insulating materials as a “green” alternative to polystyrene for hot and chilled foods; (3) macrogels, beads and capsules as carriers of nutraceuticals and micronutrients for foods and beverages to restore their nutrients after processing or give them health promoting benefits; (4) composite absorbents as filters for cleaning water; and (5) hydrogels as hydrophilic nutrient carriers for plant growth in soilless mediums.

Connecting Statement I

Chapter 2 provided a summary of literature on the different cellulose solvent systems and their dissolution mechanisms, as well as the food related applications of regenerated cellulose in food packaging, food thermal insulating materials, encapsulation of micronutrients and nutraceuticals, water treatment, and food agriculture. Among various cellulose solvent systems, sulfuric acid aqueous solvent was noticed because it can directly and rapidly dissolve cellulose with high molecular weight. It is inexpensive and could be easily disposed through neutralization, or re-used. Moreover, concentrated sulfuric acid aqueous solution is already being used in industry for preparation of cellulose nanocrystals. Hence, it is possible to use this solvent on a large scale to process cellulose waste materials into value-added products. In the research presented in chapter 3, two types of waste paper, office paper and cardboard, were converted into value-added cellulose films through rapid dissolution in pre-cooled H_2SO_4 aqueous solution. The regenerated films were a promising matrix to load antimicrobial compounds, and thus, inhibited the growth of pathogenic bacteria. Chapter 3 has been published in *Carbohydrate Polymers*: Camelia Oliva, Weijuan Huang, Souhaïla El Badri, Maria Ai Lan Lee, Jennifer Ronholm, Lingyun Chen, Yixiang Wang. Concentrated sulfuric acid aqueous solution enables rapid recycling of cellulose from waste paper into antimicrobial packaging, *Carbohydrate Polymers*, 2020, 241, 116256.

Chapter 3. Concentrated sulfuric acid aqueous solution enables rapid recycling of cellulose from waste paper into antimicrobial packaging

3.1 Abstract

Waste paper is a major contributor to municipal and industrial waste, and its recycle and reuse are a current challenge. The aim of this research is to convert waste paper into value-added cellulose films through rapid dissolution in pre-cooled H_2SO_4 aqueous solution. Two types of waste paper, office paper and cardboard, could be dissolved within 210s. The regenerated office paper films were transparent, and exhibited excellent mechanical properties (tensile strength: 77.55±6.52 MPa, elongation at break: 2.67±0.30%, and Young's modulus: 5451.67±705.23 MPa), which were comparable to those of cellulose films prepared from spruce pulp in the same solvent. The mixed paper films showed a dramatically reduced UV transmittance due to the existence of lignin. Moreover, the regenerated films were a promising matrix to load antimicrobial compounds, and thus inhibited the growth of pathogenic bacteria. Therefore, this work provides a convenient way to directly convert waste paper into biodegradable antimicrobial packaging materials.

3.2 Introduction

Cellulose is well known to be a renewable natural resource due to its abundance, availability, biodegradability, and biocompatibility (Medronho & Lindman, 2015). Currently, cellulose raw materials are mainly used for the production of paper and cardboard products, and it has been estimated that 400 million tons of waste paper are generated per year (Neelamegam et al., 2018). The majority of waste paper is disposed in landfills or subjected to incineration, which negatively affects the environment. Moreover, this is a loss of valuable cellulose raw material (Annamalai et al., 2020). Recycling waste paper back into sheets of paper and cardboards is a challenge due to the shortening of cellulose fibers, which reduces the mechanical properties of these products (Annamalai et al., 2018). Thus, there is a need in expanding more methods to re-utilize waste paper. Several attempts have been made, such as producing biofuels and sugar derivatives through biochemical conversion, obtaining cellulose nanocrystals, preparing cellulose-based absorbents for heavy metal ions and spilled oil in water, and synthesizing cyanoethyls and carboxymethyl cellulose (Annamalai et al., 2020; Li et al., 2018; Li et al., 2017; Orue et al., 2017; Zhang et al., 2015).

Cellulose is a highly-structured biopolymer held together by inter- and intra-molecular hydrogen bonds that render it insoluble in most commonly used solvents (Medronho & Lindman, 2015). Several solvent systems have been reported for cellulose dissolution, such as ionic liquids, *N*-methyl morpholine-*N*-oxide (NMMO), LiCl/*N*,*N*-dimethyl-acetamide (DMAc), and ‘green’ aqueous solvents (Chen et al., 2018; Cuissinat & Navard, 2006; Huang et al., 2016; Jiang et al., 2017; Liu et al., 2016; Minnick et al., 2016; Kim et al., 2014). Among them, it has been recently demonstrated that sulfuric acid aqueous solution could directly and rapidly dissolve spruce cellulose with relatively high molecular weight (Huang et al., 2016). As far as we know, concentrated sulfuric acid aqueous solution has been widely used to prepare cellulose nanocrystals, and the industrial production is available, so it is also possible to apply this solution into cellulose dissolution; however, its capacity to dissolve cellulose from biomass waste has been seldom reported. There is an increasing interest in developing regenerated cellulose-based films due to their environmentally friendly advantages, which in turn contribute to reducing environmental pollution as an alternative to using synthetic films (Dashipour et al., 2015). Active food packaging materials are one of many possible applications of cellulose films, in which antimicrobial agents could be incorporated to inhibit the growth of foodborne bacteria. For instance, Fu et al. reported the preparation of zinc oxide/cellulose nanocomposites through adding ZnO in NaOH/urea aqueous solution (Fu et al., 2017). The obtained films displayed good antimicrobial activity against *Staphylococcus aureus* and *Escherichia coli*, and excellent photocatalytic properties. Dashipour et al., fabricated cellulose-based films with the incorporation of *Zataria multiflora Boiss* (avishan-e shirazi) essential oil (ZEO) at different concentrations (1, 2, and 3%) (Dashipour et al., 2015). The products exhibited the improved antimicrobial and antioxidant activities with increasing the concentration of ZEO. Similar results have been reported by Tunç et al., where cellulose films loaded with carvacrol essential oil demonstrated antimicrobial activity against the selected bacteria (Tunç & Duman, 2011).

Therefore, we proposed that concentrated sulfuric acid aqueous solution is an effective solvent for recycling waste cellulose materials into value-added products. In this study, the dissolution of waste office paper, cardboard, and their mixture in H_2SO_4 aqueous solution was investigated. Cellulose films were regenerated from the aqueous solutions, and their structure and properties were studied by Fourier transform infrared spectroscope (FT-IR), X-ray diffraction (XRD), scanning electron microscope (SEM), ultraviolet-visible (UV-vis) spectroscope, and tensile test. In addition, ZnO and carvacrol essential oil were selected as the model compounds to be incorporated in cellulose films by a simple immersion, and the antimicrobial activity against gram-positive bacterium and gram-negative bacterium was evaluated. Our findings are expected to provide a facile approach to recycle cellulose from biomass waste into functional materials.

3.3 Experimental methods

3.3.1 Materials

Waste office paper (OP) and cardboard (CP) were collected from the departmental recycling bin. Sulfuric acid, sodium hydroxide and zinc oxide were purchased from Millipore Sigma (Ontario, Canada), and used without further purification. Carvacrol was kindly provided by Dr. Ashraf Ismail, Department of Food Science and Agricultural Chemistry, McGill University. Distilled water is used unless specified otherwise.

3.3.2 Waste paper dissolution and regeneration

Waste paper (4 g) was added in 96 mL 64 wt% H_2SO_4 aqueous solution pre-cooled to -20 $_oC$ with vigorous mechanical stirring (IKA® Eurostar 60 digital mixer) at 800 rpm for 5 min (Huang et al., 2016). Dissolution process of waste paper was observed and recorded by a digital camera Canon PC1339 (Canon Inc., Japan) and an optical microscope (ZEISS Primovert, Carl Zeiss, Inc., Germany) at 0, 60, 150, and 210 s after waste paper was added in H_2SO_4 aqueous solution. Then, the solutions were immediately spread onto a polytetrafluoroethylene (PTFE) plate as a 1 mm-thick layer and immersed in a coagulation bath of 10 % (w/v) NaOH aqueous solution for 10 min at 0-4 $_oC$. The resultant films were washed thoroughly with water, and then dried in air at 25 $_oC$ and coded as ROP, RMP, and RCB, corresponding to 100% waste office paper, mixed waste office paper/cardboard (4:1), and 100% waste cardboard, respectively. In order to prepare packaging materials with antibacterial property, cellulose films were regenerated in the coagulation bath containing 10 % (w/v) NaOH and 1 wt% ZnO, or the washed wet cellulose films were immersed in 1 wt% and 2 wt% carvacrol/ethanol/water solutions for 2 h. The obtained films were dried at 25 $_oC$ for 24 h (thickness: about 0.08 mm), and were coded as ROP-ZnO, ROP-1%EO, and ROP-2%EO, respectively.

3.3.3 Regenerated film characterization

In order to investigate the structure change of waste papers after dissolution and regeneration, FT-IR spectra of waste papers and regenerated films were recorded on a Nicolet 6700 spectrophotometer (Thermo Fisher Scientific Inc., Waltham, MA). The samples were vacuum-dried for 24 h prior to test and then placed on an attenuated total reflectance (ATR) accessory equipped with a Ge crystal. Spectra were recorded as the average of 64 scans at 4 cm^{-1} resolution and 25 °C, using the empty accessory as blank. X-ray diffraction (XRD) patterns were recorded on a Bruker D8 Discovery X-Ray diffractometer, using Cu Kα radiation ($\lambda = 0.154$ nm) at 40 kV and 44 mA (2θ was from 4° to 45°) with a scan rate of 1°/min. The optical transmittance (Tr) of regenerated films was measured with a S-3100 UV-vis spectrophotometer (Scinco Co. Ltd., Japan) in a wavelength range of 200-800 nm.

Morphology observation of the regenerated films was carried out with a Zeiss EVO MA10 scanning electron microscope (SEM) at an acceleration voltage of 5-10 kV. The film samples were frozen in liquid nitrogen, snapped immediately and then freeze-dried to obtain the cross-sectional fracture surface. The samples were sputtered with gold for 2 min prior to observation and photographing.

Tensile test of the regenerated films was performed by using an Instron 5967 universal testing machine (Instron Corp., MA, USA) at a crosshead speed of 5 mm min^{-1} according to standard ISO 527-2, 1993 (E). Five strips with a dimension of 5 cm × 1 cm (length × width) were cut from each film. The thickness of regenerated films was measured by a digital micrometer with a precision of 1 μm. All the films were vacuum-dried for 24 h before test.

3.3.4 Antibacterial activity test

The susceptibility of a representative Gram-positive bacterium and a representative Gram-negative bacterium to each test material was assessed using the Kirby-Bauer Disk Diffusion Susceptibility Protocol (Kirby et al., 1956-1957). Briefly, *E. coli* and *S. aureus* were grown overnight on Luria-Bertani (LB) medium solid agar in petri dishes. A sterile loop was used to touch four or five well-isolated colonies and resuspend these colonies in 2 mL of sterile saline and the turbidity of the suspension was adjusted to a 0.5 McFarland standard. A sterile swab was placed in the liquid and rotated against the inside of the tube to remove excess. The swab was used to inoculate the surface of a Mueller-Hinton (MH) agar plate. The regenerated films with or without ZnO/carvacrol were cut into small pieces circular pieces (diameter: 5 mm), sterilized by UV light and placed on the MH plates and incubated at 37 $_{o}$C for 24 h. After incubation, a bacterial inhibition zone formed around the film. The width of the inhibition zone (W_{inh}) was calculated using the following equation (Fu et al., 2015).

$$W_{inh} = (d_1 - d_2)/2 \quad (1)$$

where d_1 is the total diameter of the inhibition zone and the film, and d_2 is the diameter of the film (10 mm).

3.3.5 Statistical analysis

Experimental results were represented as the mean of five batches ± SD. Statistical evaluation was carried out by analysis of variance (ANOVA) followed by multiple-comparison tests using Duncan’s multiple-range test at the 95% confidence level. All of the analyses were conducted using SAS statistical software (SAS Institute, Inc., Cary, NC) with a probability of $p < 0.05$ considered to be significant.

3.4 Results and discussion

3.4.1 Dissolution of waste paper in H_2SO_4 aqueous solution

Fig. 3.1 Digital photographs of waste paper dissolution and regenerated films.

Fig.3.1 depicts the dissolution process and regenerated films. It was observed that the dissolution process for both raw materials was rather quick. The solution of waste cardboard was darker than office paper solution. A possible explanation for this is the lignin content giving a darker color to the waste cardboard solution. It was reported that A4 copy paper sheets contain about 73% of fully bleached chemical pulp and 27% of inorganic material analyzed as ash content, and the cardboard was a mixture of mechanical, semi-chemical and chemical pulps having a high lignin content of over 10% (Ma et al., 2016**).** Three types of films (ROP, RMP and RCB) were successfully regenerated through basic coagulation bath. It indicated that the pre-cooled H_2SO_4 aqueous solution was efficient to convert waste paper into cellulose films without any pre-treatments, even when the waste was a mixture. As shown in Fig. 3.1, ROP film was transparent and colorless. The presence of small amounts of waste cardboard in RMP led to a light brown film but still transparent, while RCB film was translucent and had a dark color due to its high lignin content.

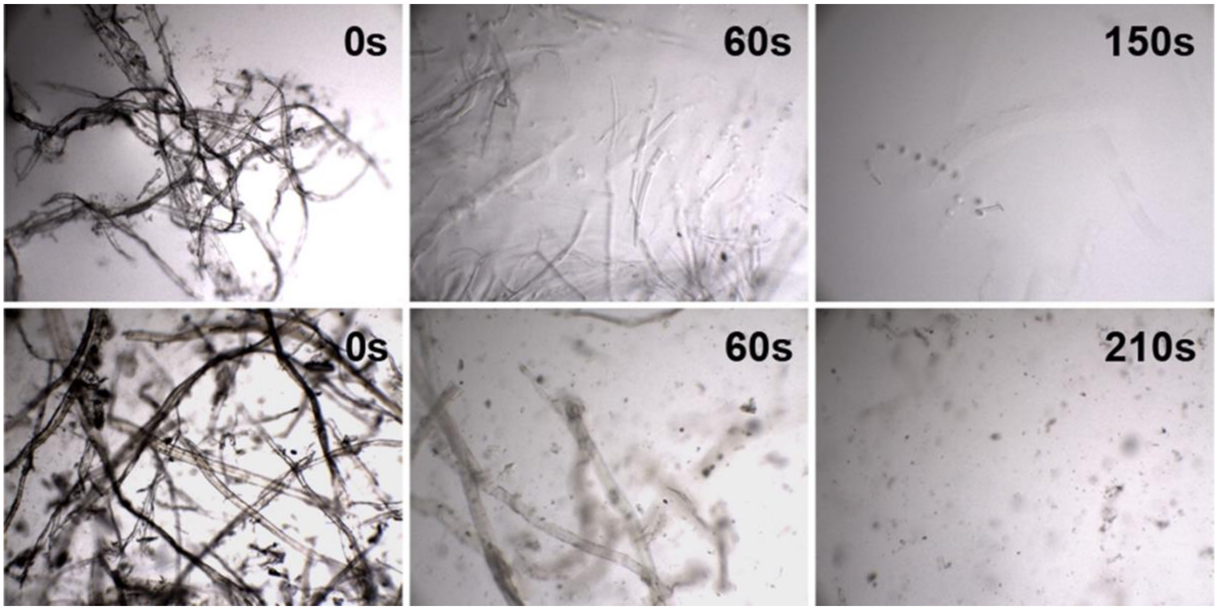

Fig. 3.2 Optical microscopic images of dissolution process at 0, 60, 150, 210 s of waste paper in 64 wt% H_2SO_4 aqueous solution pre-cooled to -20 $_o$C: OP (top row) and CB (bottom row).

To better visualize the dissolution process of waste office paper and cardboard in 64 wt% H_2SO_4 aqueous solution pre-cooled to -20 $_o$C, optical microscopic images of waste paper fibers in solution were taken at 0, 60, 150, 210 s of dissolution. As shown in Fig.3.2, waste paper fibers were dispersed in H_2SO_4 aqueous solution at 0 s, and then became semi-transparent after 60 s. It meant that these fibers swelled and began to disappear at a very early stage, revealing the nature of rapid dissolution. It was worth noting that OP fibers almost disappeared at 150 s, whereas for CB sample, tiny undissolved pieces still remained at 210 s. Nishiwaki-Akine et al. studied the dissolution of wood cellulose in formic acid, and found that the lignin content present in wood raw materials greatly affected the solubility of cellulose (Nishiwaki-Akine et al., 2017). Moreover, compared to CB, more chemical and mechanical treatments were performed during the production of OP, which caused damages to OP fibers, so the dissolution of CB took slightly more time. As far as we know, the concentrated H_2SO_4 aqueous solution is usually used to hydrolyze cellulose to prepare cellulose nanocrystals (Wang & Chen, 2011). In our previous study, spruce cellulose (bleached Kraft pulp) could be dissolved in 120 s **(**Huang et al., 2016); and now, it is demonstrated again the pre-cooled H_2SO_4 aqueous solution is a promising solvent of waste paper cellulose.

3.4.2 Structure and properties of regenerated waste paper films

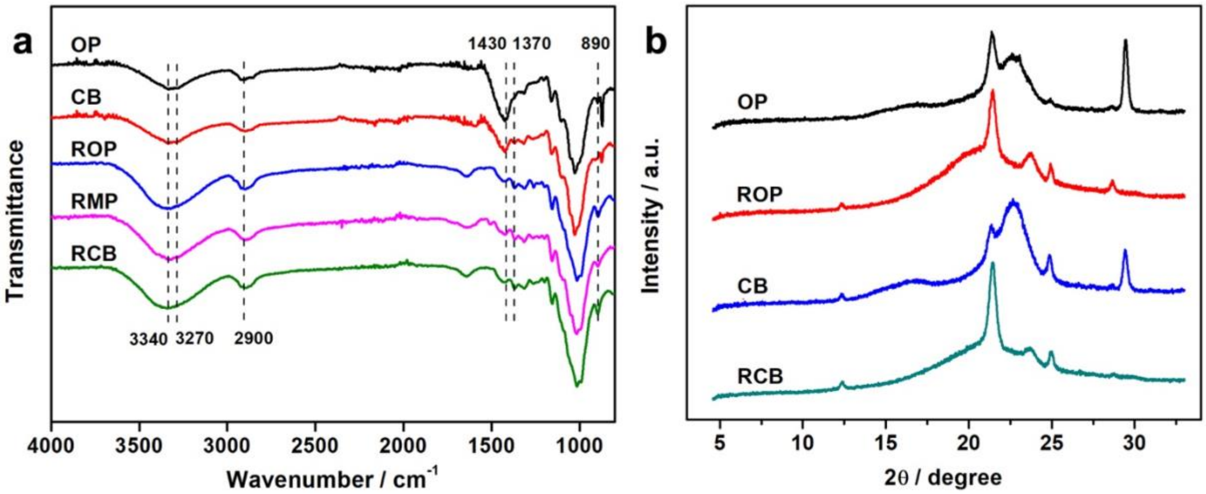

Fig. 3.3 (a) Fourier transform infrared spectra and (b) X-ray diffraction patterns of waste paper and regenerated films.

To investigate the structure change of cellulose in waste paper after dissolution and regeneration, FT-IR spectra were obtained. As shown in Fig. 3.3a, all the samples displayed the similar characteristic IR absorption peaks as no new peaks were apparent. It indicated that there was no cellulose derivative generated during dissolution and regeneration. However, slight changes were observed when the spectra of waste paper and regenerated films were compared. For both OP and CB samples, the peak at 1430 cm^{-1} is due to a crystalline absorption, and the absorbance ratio of the bands at 1430 and 900 cm^{-1} (I_{1430}/I_{900}), adopted as crystallinity index (CI), is closely related to the portion of cellulose I structure (Oh et al., 2005). After dissolution and regeneration, the ratios of I_{1430}/I_{900} decreased, which indicated a loss of crystallinity (Alves et al., 2015). Similar results have been reported in our previous work that the CI values of original spruce cellulose sample and regenerated cellulose film were 59% and 43%, respectively, accompanying with a transition from cellulose I to cellulose II structure (Huang et al., 2016). In Figure 3a, both OP and CB samples showed the characteristic peaks of cellulose I at 3270 and 3340 cm^{-1}. The absorption band at 3270 cm^{-1} was not obvious in the regenerated cellulose films, and the OH peak broadened, suggesting the change of cellulose polymorph and the reduction of cellulose crystallinity (Kafle et al., 2014). The change in cellulose polymorph was further confirmed by the X-ray analysis. As shown in Fig. 3.3b, the starting OP and CB materials presented a major diffraction centered at ca. 22.5° (200) and two other characteristic reflections at 15.0° ($1\bar{1}0$) and 16.6° (110), which were typical for a cellulose I crystalline organization (Alves et al., 2016). These peaks disappeared and a new broad diffraction at about 20.6° was observed when cellulose was dissolved in H_2SO_4 aqueous solution and regenerated. It indicated that the crystalline structure changed to a cellulose II type arrangement (Li et al., 2015). It was worth noting that some other diffraction peaks existed, which might be attributed to the fillers and additives in paper (Causin et al., 2010). Some of them could be removed after dissolution and washing, for example, the intensity of peak at 29.6° (might relate to the crystallite form of calcite) decreased considerably (Orue et al., 2017), while some compounds were wrapped in cellulose matrix during regeneration. Transparency is an important feature of packaging materials. Fig. 3.4 shows the ultraviolet-visible (UV-vis) transmittance of regenerated waste paper films. It was observed that the ROP film displayed a relatively high transmittance (70-80%) in the wavelength range between 400 to 800 nm. The presence of waste CB in RMP sample led to a decrease in film transparency compared to that of ROP film, which slightly dropped to about 71% at 800 nm. However, the transmittance of RMP film in the wavelength range between 200 to 400 nm dramatically reduced, suggesting that it could absorb or block a certain portion of UV light. The RCB film was translucent with a transparency of about 50% at 800 nm, but it was an excellent UV light barrier. Sadeghifar et al. studied the UV protection property of cellulose-lignin films (Sadeghifar et al., 2016). It was demonstrated that lignin is an excellent light absorber in the range of 190-400 nm due to its aromatic phenolic structure (Sadeghifar et al., 2016). With the addition of 2% lignin, the cellulose film absorbed all UV-B light (280-320 nm) and the majority of UV-A light (320-340nm) (Sadeghifar et al., 2016). Therefore, the reduced transparency of RMP and RCB samples was caused by the presence of lignin and tiny undissolved pieces. The ROP film could be used as transparent packaging material, while waste CB could be applied as an additive to fabricate UV light barrier.

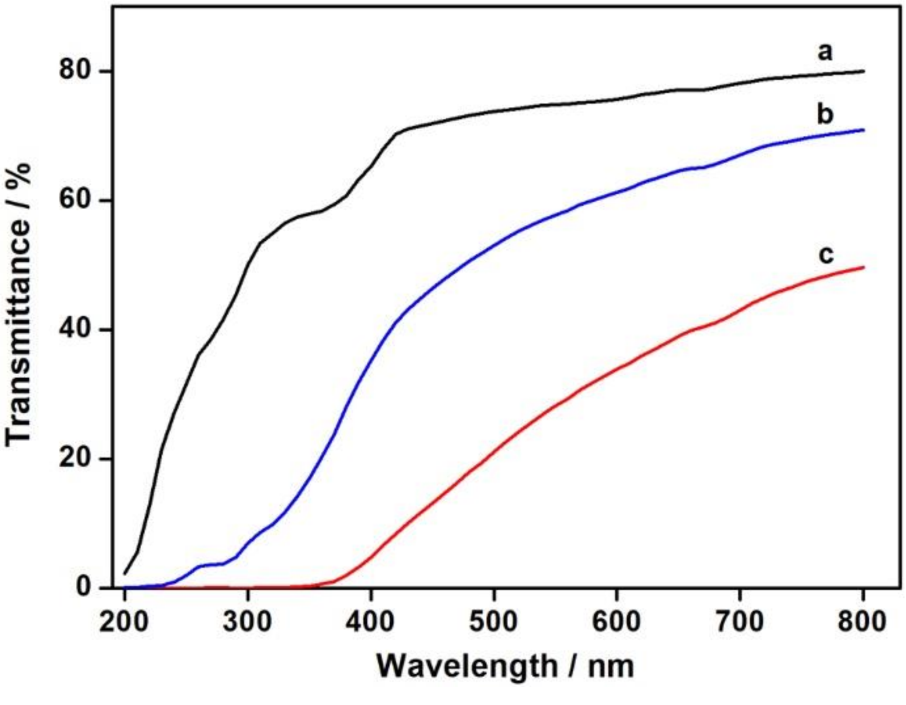

Fig. 3.4 Ultraviolet visible transmittance of regenerated waste paper films: (a) ROP, (b) RMP, and (c) RCB.

In order to further reveal the microstructures of regenerated waste paper films, the surfaces and cross-sections were observed by scanning electron microscope (SEM). As shown in Fig. 3.5a and Fig. 3.5d, the ROP film had the relatively smooth and uniform structure. It was because of the successful dissolution of waste OP in pre-cooled H_2SO_4 aqueous solution. During the regeneration process, the solvent was replaced by a cellulose non-solvent to trigger a phase separation, for example, concentrated sulfuric acid was diluted or neutralized. Therefore, abundant hydrogen bonding and hydrophobic interactions were then "switched-on" among amphiphilic cellulose molecules to form the films (Medronho et al., 2012; Wang & Chen, 2011). It was worth noting that aqueous solutions were chosen as the solvent and non-solvent to avoid the usage of organic solvents in this study. In Figs. 3.5b, 3.5e, 3.5c, and 3.5f, an intact structure was also observed for RMP and RCB films, but their surfaces and cross-sections were not as smooth as those of ROP. Particulate structures existed in the samples, which might be attributed to the presence of tiny undissolved pieces from waste CB.

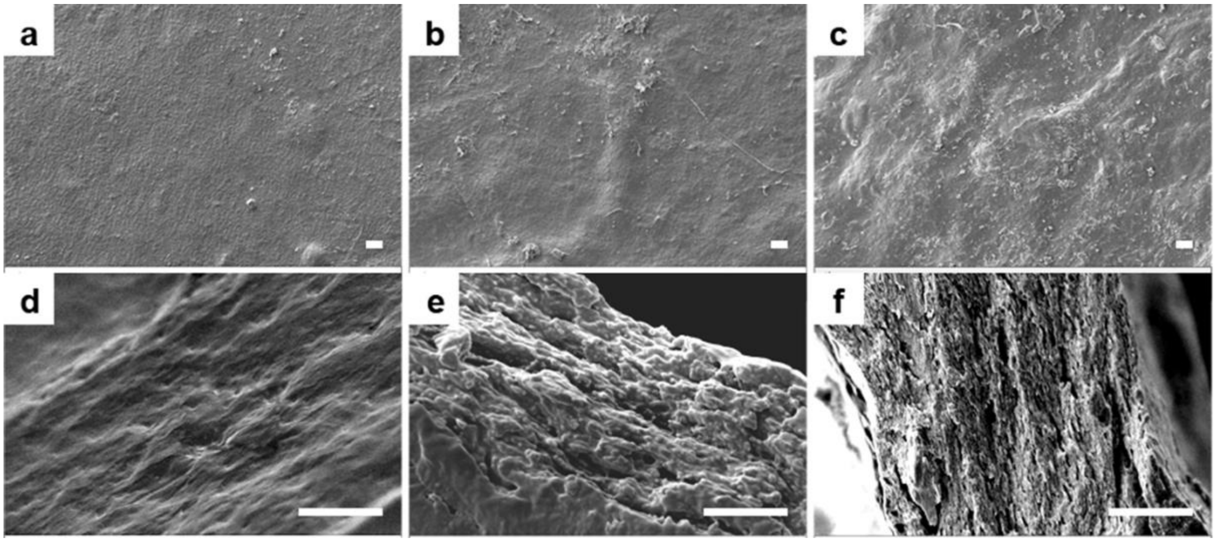

Fig. 3.5 SEM images of the surfaces (top) and cross-sections (bottom) of regenerated waste paper films: (a, d) ROP, (b, e) RMP, and (c, f) RCB. Scale bar = 10 μm.

Mechanical properties of regenerated waste paper films were studied by tensile test. The tensile strength, elongation at break, and Young's modulus of ROP films were 77.55 ± 6.52 MPa, 2.67 ± 0.30%, and 5451.67 ± 705.23 MPa, respectively, which were comparable to those of cellulose films prepared from spruce pulp in the same solvent (Huang et al., 2016). It was noticed that the spruce cellulose films were prepared from 2% (w/v) cellulose solution, while the content of waste paper was 4% (w/v) in this study. Aforementioned in the introduction, recycling waste paper and carboard back into sheets of paper is challenging because their mechanical properties maybe compromised due to fiber shortening (Annamalai et al., 2018). However, this shortcoming could be compensated by increasing the concentration of waste paper in solution to fabricate the regenerated films with similar mechanical properties as sheets of paper. For RMP and RCB films, their tensile strength, elongation at break, and Young's modulus decreased compared to those of ROP films. It was because of the presence of tiny undissolved pieces in the films, which acted as the structural defects and affected the mechanical properties. Similar phenomenon has been reported by Sadeghifar et al., with the addition of 2% lignin (Sadeghifar et al., 2016). However, the tensile strength and Young's modulus of RMP and RCB films were still comparable to those of isotactic polypropylene, recycled polyethylene terephthalate/recycled polypropylene, and polypropylene/polyethylene copolymers (Li et al., 2019; Marzuki et al., 2018; Palange et al., 2019).

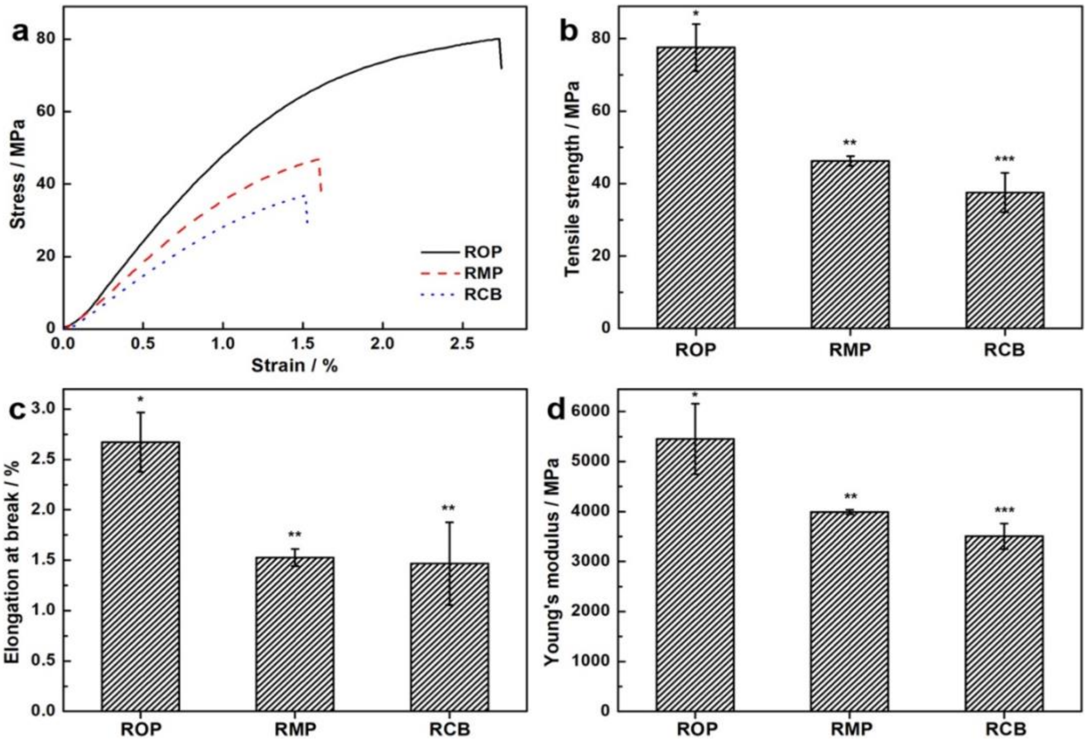

Fig. 3.6 Mechanical properties of regenerated waste paper films. Different asterisks on the top of the columns indicate the significant difference ($p < 0.05$).

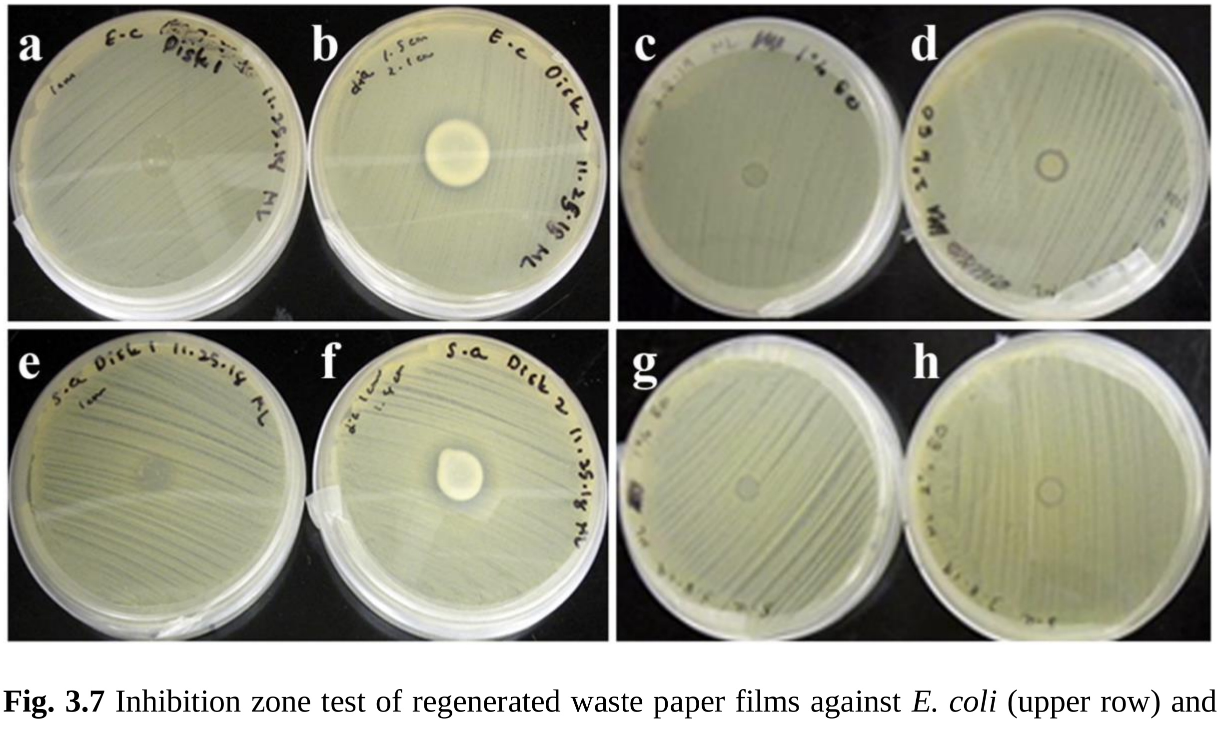

Fig. 3.7 Inhibition zone test of regenerated waste paper films against *E. coli* (upper row) and *S. aureus* (bottom row): (a, e) ROP, (b, f) ROP-ZnO, (c,g) ROP-1%EO, and (d, h) ROP-2%EO.

The porous structure of regenerated cellulose films (wet) provides a promising matrix to load active compounds (Wang et al., 2017). In this study, ROP films were transparent and had good mechanical properties, so they were chosen to prepare active packaging materials. ZnO and carvacrol essential oil were incorporated into ROP films, and their antimicrobial property against *E. coli* and *S. aureus* is shown in Fig. 3.7 No inhibition zone was observed for ROP films because they served as the control, but all the other samples exhibited a certain level of capacity to inhibit the growth of bacteria. For ROP-ZnO films, the inhibition zones against *S. aureus* and *E. coli* were 2.0 cm and 1.2 cm, respectively. Similar inhibition effects were reported for ZnO loaded amidoximated wool fibers electrospun gelatin/ZnO fibers and electrospun polycaprolactone /hydroxyapatite/ZnO nanofibers (Chen et al., 2019; Ma et al., 2019; Shitole et al., 2019)**.** It was noticed that the inhibition zones of ROP-EO films were not as large as those of ROP-ZnO samples, but the size of the zones recognizably increased when the content of EO rose from 1% to 2%. This was because the antimicrobial effect of EO depended on the release from film matrix, and an adequate EO vapor concentration was necessary to achieve the inhibition against *S. aureus* and *E. coli* bacteria (Tunç & Duman, 2011)**.** Therefore, our study revealed that it was possible to incorporate antimicrobial agents into regenerated waste paper by a simple immersion to fabricate active packaging materials.

3.5 Conclusion

The pre-cooled sulfuric acid aqueous solution was an efficient solvent that could rapidly dissolve waste office paper and cardboard and subsequently convert them into regenerated cellulose films. The dissolution of waste CB was relatively slower than that of OP, and several tiny undissolved pieces of CB were observed in the solution, which might be attributed to its high lignin content. However, it was worth noting that the presence of waste CB in the films largely improved the UV light barrier property. Due to the successful dissolution, the ROP films were transparent and uniform, and exhibited the similar mechanical properties compared to those of cellulose films prepared from spruce pulp in the same solvent, which overcame the challenge in recycling waste paper caused by the shortening of cellulose fibers. The tensile strength and Young's modulus of RMP and RCB films were also comparable to those of some synthetic plastics. Moreover, the regenerated cellulose films could act as a porous matrix to load antimicrobial compounds for the fabrication of active packaging materials. Therefore, this work promoted the application of concentrated sulfuric acid aqueous solution in recycling cellulose from waste materials. Considering the availability of industrial scale production of cellulose nanocrystals using concentrated sulfuric acid, the large scale utilization of this solution is possible. Further studies on the requirement of temperature and reuse of chemicals will be carried out to make the dissolution more sustainable and cost effective.

Connecting Statement II

Chapter 3 reported that the pre-cooled sulfuric acid aqueous solution was an efficient solvent to rapidly dissolve waste office paper and cardboard and subsequently convert them into regenerated cellulose films. It was noticed that the resultant cellulose solution was not quite stable at room temperature due to the hydrolysis of cellulose by concentrated sulfuric acid. Therefore, in order to develop cellulose hydrogel beads with potential application in agriculture (MSSI Innovation project), Chapter 4 employed NaOH/urea aqueous solvent to dissolve waste paper to obtain a relatively stable cellulose solution, which allowed the fabrication of regenerated cellulose beads through a simple drop-wise syringe extrusion method. Chapter 4 will subsequently be submitted as a manuscript for publication in *Journal of Agricultural and Food Chemistry*: Camelia Oliva, Yixiang Wang. Recycling of wastepaper into cellulose hydrogels for water and fertilizer savings in dryland agriculture, *Journal of Agricultural and Food Chemistry*, 2020, to be submitted.

Chapter 4. Recycling of wastepaper into cellulose hydrogels for water and fertilizer savings in dryland agriculture

4.1 Abstract

Waste office paper was recycled by dissolving in NaOH/urea aqueous solution and then regenerated into cellulose hydrogels as a biodegradable matrix for controlled release fertilizer, and at the same time, store water for dryland agriculture. The structure and properties of obtained cellulose hydrogels were studied by ATR-FTIR, XRD, SEM, re-swelling test, and fertilizer release test. The results revealed that, after pre-hydrolysis, waste office paper could be partially dissolved in NaOH/urea aqueous solution at -12.6 $_{o}$C within 15 min, and formed cellulose beads after regeneration via a simple syringe extrusion in the 10 wt% sulfuric acid coagulation bath. The crystalline structure of cellulose changed from cellulose type I to cellulose type II during dissolution and regeneration. The obtained cellulose beads had porous structure and could successfully load fertilizer (freeze-dried beads: 143.3 ±8.52 mg/g and oven-dried beads: 127.9 ±2.56 mg/g). Moreover, the hydrophilic matrix of cellulose hydrogels enabled the absorption of water in their three-dimensional network. Two different drying methods, namely freeze drying and oven drying, did not show a significant effect on the amounts of N-P-K fertilizer released from the cellulose beads (freeze-dried beads: N: 56.8 ±3.92 mg/g, P: 49.7±3.82 mg/g and K: 36.8±1.38 mg/g and oven-dried beads: N: 49.7±0.726 mg/g, P: 44.1±1.70 mg/g and K: 34.1±1.11 mg/g). However, the re-swelling ratio of freeze-dried beads (415.62±18.13 %) was recognizably higher than that of oven-dried beads (224.16±5.51%), as freeze-dried beads could re-swell 185.4% more times in water than the oven-dried beads. Therefore, this work provided a “green” method to recycle wastepaper into biodegradable porous materials with potential application in agriculture.

4.2 Introduction

According to FAO, Canada and the US produce 166 million tonnes of pulp and paper annually (FAO, 2018). After their use, a large amount of wastepaper is generated. It is generally considered that paper is recyclable; however, in fact, wastepaper can only be recycled for 2.4 times, because the cellulose fibres in paper become too short and worn out and cannot be reused to produce new paper sheets or cardboard boxes (Zhang et al., 2015). Hence, a significant amount of wastepaper ends-up in landfills or is incinerated, which has a negative impact on the environment and is a loss of underutilized cellulose-rich material (Li et al., 2017). It is predicted that there will be a rise in population of about 20% (1.4 billion) in next two decades, so the largely increased consumption of goods will be inevitable, which will ensue more waste production including waste papers (Ma et al., 2016). Therefore, new methods are needed to reuse or recycle waste papers (Orue et al., 2017). Several attempts have been recently reported to recycle wastepaper into value-added commodities, for example, the production of bioethanol by hydrolyzing wastepaper (Dubey et al., 2012), the conversion to bio-oil via pyrolysis (Zhang et al., 2015), the upcycling into prototype textiles (Ma et al., 2016), the fabrication of compressible conductive carbon aerogels (Li et al., 2017), the isolation of cellulose nanocrystals (CNC) via alkali solution and acid hydrolysis (Orue et al., 2017), and the regeneration into composite aerogel absorbents for removal of heavy metal ions in water (Li et al., 2018). Among them, the dissolution of wastepaper in “green” solvents to regenerate it into functional materials is a promising way. It has been recognized that NaOH/urea aqueous system is cheap, non-volatile, and nontoxic, and can efficiently dissolve cellulose (Han et al., 2015; Jiang et al., 2014; Li et al., 2018; Zhang et al., 2017; Zhang et al., 2016). However, the application of this “green” solvent in recycling wastepaper has been seldom reported.

Hydrogels are three-dimensional networks that are rich in hydrophilic polymers and can absorb and sustain significantly large amounts of water (Chang et al., 2010). They can be prepared from different types of polymers, and the network can be constructed by chemical crosslinking, physical entanglement, and rearrangement of ionic and hydrogen bonds (Chang et al., 2010). For example, cellulose hydrogels can be fabricated by two different modes: 1) chemical crosslinking, where cellulose or cellulose derivatives (i.e. cellulose acetate, hydroxyethyl cellulose, and carboxymethyl cellulose) are crosslinked via a di-functional molecule (i.e. epichlorohydrin (ECH)) (Zhou et al., 2007); and 2) physical crosslinking, where non-derived cellulose can be crosslinked via rearrangement of their intra- and intermolecular hydrogen bonds (Wang & Chen, 2011). Due to the abundant hydrophilic hydroxyl groups on cellulose molecular chains and the porous structure, cellulose hydrogels can store certain amounts of water and load with bioactive molecules. In turn, they can serve as carrier vessels for controlled-release of loaded compounds at the targeted sites and/or in desired environments. For example, a sustainable release of bovine serum albumin (BSA) in simulated body fluid was achieved from cellulose nanowhisker composite hydrogels as biomedical drug delivery systems (Wang & Chen, 2011); celery cellulose hydrogels could deliver short-chain-fatty acids (SCFAs) upon ultrasound-triggered strategy (Yan et al., 2020); composite cellulose-based hydrogels could be used as nutrient and water reservoirs to improve crop irrigation and fertilizer conservation capacity of soil (Calcagnile et al., 2019; Wang et al., 2020; H. Zhang et al., 2017). However, the application of cellulose hydrogels regenerated from upcycled wastepaper in agriculture has never been investigated.

In this work, we intended to dissolve waste office paper in “green” NaOH/urea aqueous solvent system and regenerate cellulose hydrogel beads. Subsequently, commercial N-P-K fertilizer was loaded in cellulose beads by simply immersing them in fertilizer solutions. Two drying methods, namely oven drying and freeze-drying, were applied, and the structure and properties of cellulose beads with or without fertilizer were investigated in detail.

4.3 Experimental methods

4.3.1 Materials

Waste office paper (OP) were collected from the departmental recycling bin from Department of Food Science and Agricultural Chemistry, McGill University. Sulfuric acid, sodium hydroxide, and urea were purchased from Millipore Sigma (Ontario, Canada), and used without further purification. Commercial N-P-K fertilizer (20-20-20) was provided by Dr. Madramootoo in the Department of Bioresource Engineering, McGill University.

4.3.2 Wastepaper pre-treatment

Since NaOH/urea aqueous solvent can only dissolve cellulose with molecular weight lower than 1.0×10^5, waste office paper was pre-treated by acid hydrolysis according to Gong et al.'s method with some modifications (Gong et al., 2014). In brief, 130 g waste office paper (OP) was placed in 1000 mL of 15 wt% H_2SO_4 (aq), and the suspension was stirred at room temperature for 24 h. Subsequently, the hydrolyzed paper (HP) was isolated by vacuum filtration and washed several times with distilled water to achieve a neutral pH, which was tested with litmus paper. Afterwards, HP was oven-dried at 50^oC for 24 h, and grinded to obtain a final weight of 114.5g.

4.3.3 Hydrolyzed paper (HP) dissolution and regeneration

The aqueous solvent was prepared by dissolving 7 g NaOH and 12 g urea in 81 mL water. Subsequently, 4 g HP was added to 96 mL NaOH/urea solution and mixed at 1000 rpm for 2 min. The suspension was placed in the freezer overnight (-20^oC), and then thawed-out to a temperature of -12.6^oC and stirred at 2000 rpm for 15 min to obtain a semi-viscous liquid solution (Gong et al., 2014). Cellulose solution was regenerated into hydrogel beads by drop-wise syringe extrusion in a 10 wt% H_2SO_4 aqueous coagulation bath at 0-4 $_o$C. After 10 min, hydrogel beads were filtered out of coagulation bath and washed with distilled water until they reached a neutral pH, which was tested with litmus paper.

4.3.4 Cellulose hydrogel beads loaded with commercial fertilizer

The obtained cellulose hydrogel beads were immersed in a 10% (w/v) commercial N-P-K fertilizer (CF) solution for 24 h. Cellulose beads loaded with fertilizer were then separated and dried by two methods: 1) oven-drying and 2) freeze-drying, respectively. For oven drying, the beads were placed in a conventional oven at 50$_o$C for approximately 4 days. For freeze-drying, the samples were stored in a freezer at -20$_o$C overnight, and then put into the freeze-drier for approximately 36 h. The resultant dry hydrogel beads were coded as follows: 1) empty oven-dried beads without fertilizer (OE); 2) empty freeze-dried beads without fertilizer (FE); 3) oven-dried beads loaded with fertilizer (OD); and 4) freeze-dried beads loaded with fertilizer (FD).

4.3.5 Cellulose hydrogel beads characterization

In order to investigate the structure change of waste office paper during dissolution and regeneration, FT-IR spectra of waste office paper and regenerated cellulose beads were recorded on a Nicolet 6700 spectrophotometer (Thermo Fisher Scientific Inc., Waltham, MA). The samples were vacuum-dried for 24 h prior to test and then placed on an attenuated total reflectance (ATR) accessory equipped with a Ge crystal. Spectra were recorded as the average of 64 scans at 4 cm$_{-1}$ resolution and 25 °C, using the empty accessory as blank. X-ray diffraction (XRD) patterns were recorded on a Bruker D8 Discovery X-Ray diffractometer, using Cu Kα radiation (λ=0.154 nm) at 40 kV and 44 mA (2θ was from 4° to 45°) with a scan rate of 1°/min.

Morphology observation of the regenerated cellulose beads with or without commercial fertilizer was carried out with a TM 3000 Table Top Hitachi scanning electron microscope (SEM) at an acceleration voltage of 5 kV. SEM images were taken at 50x and 3000x respective magnifications.

Re-swelling ratio (RSR) of OE and FE samples was determined to evaluate the water absorption capacity of cellulose hydrogel beads. Both samples (0.1 ± 0.0001g) were immersed in 14 mL distilled water for 3 days at room temperature to reach the equilibrium. Subsequently, they were separated and weighed after wiping the surface water. The RSR is defined as:

$$\mathrm{RSR}\ (\%) = \frac{W_s}{W_d} \times 100 \tag{1}$$

Where W_d is the dry weight of the regenerated hydrogel beads and W_s is the weight of the wet hydrogel beads (Zhou et al., 2007).

The amount of fertilizer loaded in regenerated hydrogel beads was determined by two methods: 1) A gravimetric analysis in monitoring the weight change of loaded and washed beads was done to determine an estimated amount of NPK fertilizer salt in cellulose hydrogel beads. The cellulose hydrogel beads loaded with fertilizer (OD & FD) were washed in distilled water at room temperature for 3 days. The change in dry weight before and after washing was monitored, and the amount of fertilizer was calculated as:

$$\text{Fertilizer loaded in beads (mg/g)} = \frac{(W_o - W)}{W} \times 10^3 \tag{2}$$

Where W_o is the initial dry weight of the regenerated hydrogel beads loaded with fertilizer, and W is the dry weight of hydrogel beads after washing; and 2) To compare to the gravimetric analysis and have a more precise determination of nitrogen (N) , phosphorus (P) and potassium (K) nutrient content being released, the cellulose hydrogel beads were measured by atomic absorption elemental analysis. OD and FD samples were weighed (0.1 ± 0.0001g), and then immersed in 50 mL distilled water for 4 days to allow the release of loaded fertilizer from beads into water. The amount of fertilizer was represented by the contents of N-P-K. The total released N and P were analyzed colorimetrically on the flow injection instrument (FIA Lachat QuickChem 8000). The P content was measured at 880 nm following a complexation with ammonium molybdate and ascorbic acid, while the total N was converted in the ammonium form and was measured at 660 nm by complexing with salicylate and hypochlorite in an alkaline phosphate buffer. The total K content was measured by the emission on a flame atomic absorption spectrophotometer Varian 220 FS (Agilent, USA) using same background matrix as standards and adding La and Cs for counteracting interferences and ionization (Parkinson & Allen, 1975).

4.3.6 Statistical analysis

Experimental results were represented as the mean of triplicate batches ± SD. Statistical evaluation was carried out by analysis of variance (ANOVA) followed by a one-way multiple-comparison tests using Turkey HSD test at the 95% confidence level. All of the analyses were conducted using SAS statistical software (SAS Institute, Inc., Cary, NC) with a probability of $p < 0.05$ considered to be significant.

4.4 Results and discussion

4.4.1 Waste office paper dissolution and regeneration

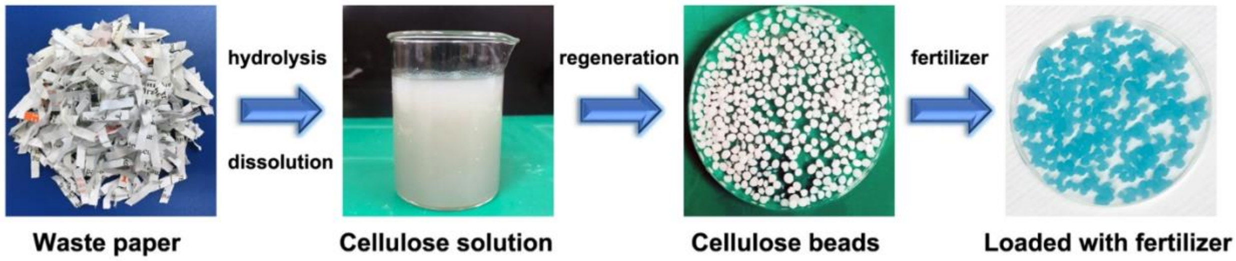

Fig. 4.1 Digital photographs of waste office paper dissolution and regenerated beads with or without loaded fertilizer.

Fig. 4.1 depicts the dissolution of waste office paper (OP) and regenerated cellulose hydrogel beads with or without loaded commercial N-P-K fertilizer. Different from our previous work, NaOH/urea aqueous solvent was selected to dissolve waste office paper, because it is a more stable system for cellulose hydrogel bead preparation compared to the concentrated sulfuric acid solution. However, NaOH/urea aqueous solvent is only efficient when the molecular weight of cellulose is lower than $1\text{x}10_5$, so the pre-treatment of acid hydrolysis with 15 wt% sulfuric acid for 24 h was carried out to decrease the molecular weight of cellulose in waste office paper (Gong et al., 2014). The hydrolyzed waste office wastepaper (HP) was then dissolved in NaOH/urea aqueous solvent at -12.6 $_{o}$C within 15 min, and a semi-viscous solution was obtained. Subsequently, cellulose hydrogel beads were regenerated dropwise through simple syringe extrusion. This step required a relatively stable solution at room temperature, but cellulose would be rapidly hydrolyzed in concentrated sulfuric acid at 25 $_{o}$C, so NaOH/urea aqueous solvent was more suitable, in this work. Cellulose hydrogel beads with uniform shape and a diameter of about 4 mm were successfully regenerated. After soaking the beads in 10 % (w/v) commercial fertilizer solution, no obvious changes in shape and size were apparent, suggesting the beads were stable, while the blue color indicated that the fertilizer was loaded in the three dimensional network of cellulose hydrogels.

4.4.2 Cellulose hydrogel beads structure

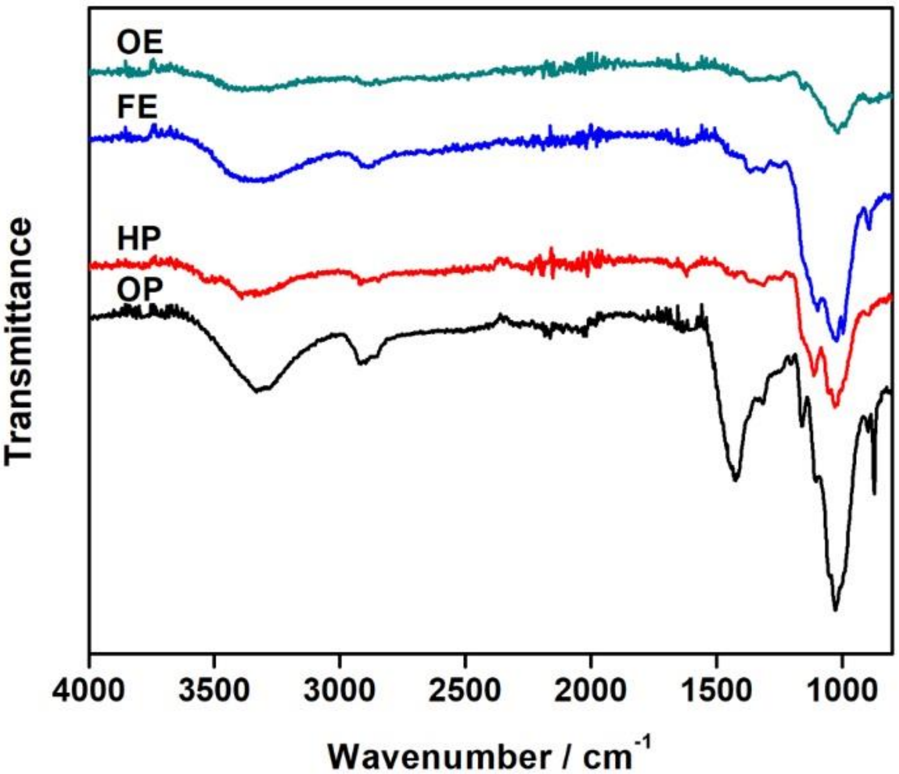

Fig.4.2 Attenuated total reflectance Fourier transform infrared spectra (ATR-FTIR) of waste office paper (OP), hydrolyzed paper (HP), empty freeze dried cellulose beads (FE), and empty oven dried cellulose beads (OE).

ATR-FTIR spectra of waste office paper (OP), hydrolyzed paper (HP), empty freeze dried cellulose beads (FE), and empty oven dried cellulose beads (OE) are shown in Fig. 4.2. It was observed that all characteristic IR absorption peaks of OP were maintained and no new peaks appeared, suggesting that no cellulose derivatives were generated during dissolution, regeneration and drying process. However, several changes in peak intensity were observed when the spectra of OP and regenerated hydrogel beads were compared. For OP sample, the peak at 1430 cm^{-1} is due to a crystalline absorption, and the absorbance ratio of the bands at 1430 and 900 cm^{-1} (I_{1430}/I_{900}), adopted as crystallinity index (CI), is closely related to the portion of cellulose I structure (Oh et al., 2005). After dissolution and regeneration, the peak intensity at 1430 cm^{-1} as well as the ratio of I_{1430}/I_{900} decreased, which indicated a loss of crystallinity (Alves et al., 2015). At the same time, the absorption bands of OP and HP at 3340 cm^{-1} shifted to higher wavenumbers and broadened after dissolution and regeneration, indicating the rearrangement of hydrogen bonds in cellulose structure and the change of cellulose polymorph (Kafle et al., 2014). It was worth noting that the spectra of OE and FE were same, which meant the two drying processes did not cause any difference in cellulose bead structures.

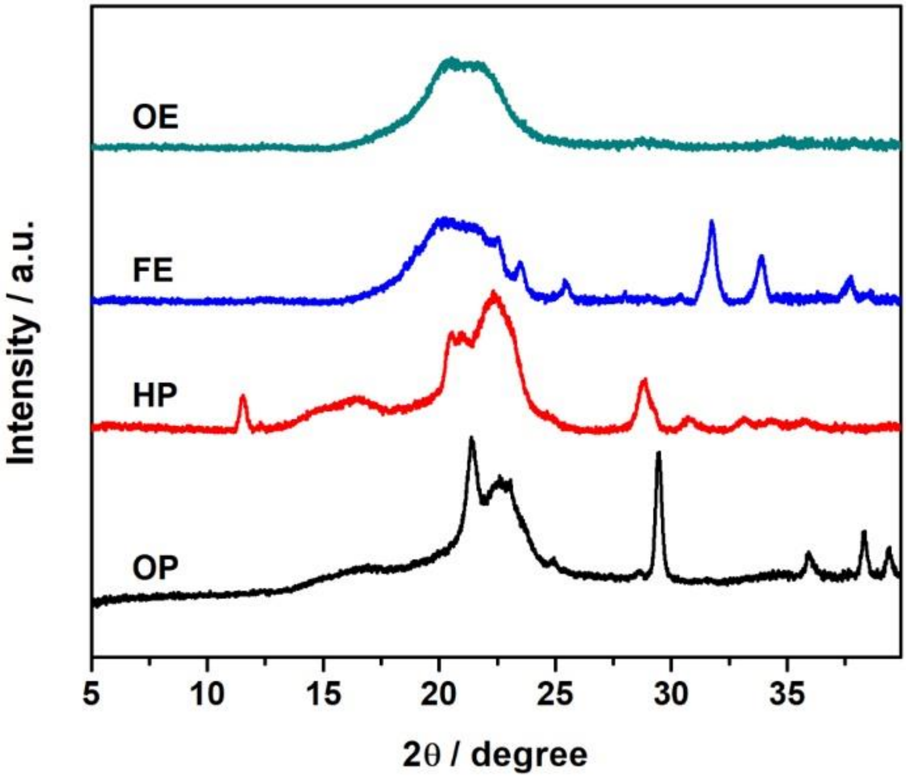

Fig. 4.3 X-ray diffraction patterns of waste office paper (OP), hydrolyzed paper (HP), freeze dried cellulose beads (FE), and oven dried cellulose beads (OE).

In order to confirm the change in cellulose crystalline structure after dissolution and regeneration, the X-ray diffraction (XRD) patterns of waste office paper (OP), hydrolyzed paper

(HP), freeze dried cellulose beads (FE), and oven dried cellulose beads (OE) are shown in Fig. 4.3 Prior to dissolution and regeneration process, OP and HP had a major diffraction peak centered at $2\theta = 22.5_o$ (200) and two other reflection peaks at $2\theta = 15.0_o$ ($1\bar{1}0$) and $2\theta = 16.6_o$ (110), which are characteristic diffraction patterns of cellulose I crystalline organization (Alves et al., 2016). For FE and OE samples, these peaks changed and a new broad diffraction at about $2\theta = 20.6_o$ was observed, which indicated a transition from cellulose type I to cellulose type II (Li et al., 2015). Some other diffraction peaks also existed in the patterns, which may be attributed to the fillers and additives in office paper (Causin et al., 2010). A certain amount of them were removed during pre-treatment, dissolution, regeneration and washing process, but some compounds were wrapped in cellulose matrix during regeneration and drying. For example, the peak at about $2\theta = 29.6_o$ in OP diffractogram completely disappear in the hydrogel bead (FE & OE) patterns. A possible additive for this peak might be the crystallite form of calcite. This is because Orue et al. reported similar XRD results in their findings, where with NaOH treatments of office waste paper, it removed impurities, such as crystallite calcite which was identified as the peak at about $2\theta = 29.6_o$ (Orue et al., 2017). In addition, the new peaks at about $2\theta = 31.7_o$ and 34.0_o in FE pattern might be the formation of inorganic salt crystals triggered by freeze-drying.

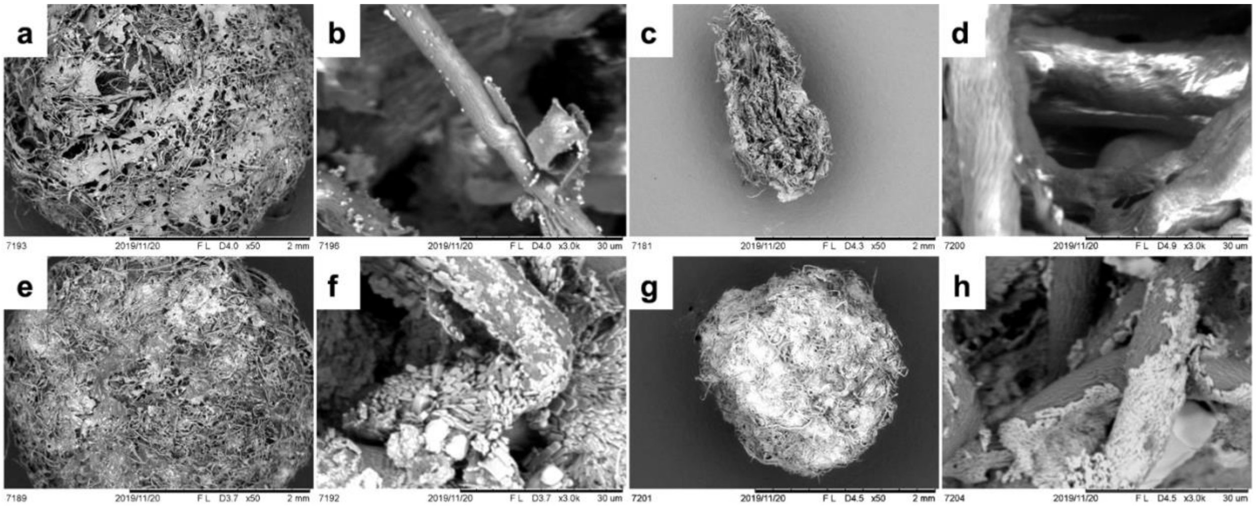

Fig.4.4 SEM images of freeze dried cellulose beads (a,b,e,f) and oven dried cellulose beads (c,d,g,h) without fertilizer (top) and loaded with fertilizer (bottom).

The micro-structures of regenerated cellulose hydrogel beads with or without loaded fertilizer were observed by scanning electron microscope (SEM). As shown in Fig. 4.4, both freeze-dried and oven-dried cellulose beads had a porous structure, which was important to load compounds, such as fertilizer, in cellulose matrix and controlled-release them. It also provided the space to absorb and reserve water due to the hydrophilic property of cellulose. It was noticed that both the diameter and pore size of FE were larger than those of OE. These differences could be attributed to the drying methods. Chang et al. reported the similar difference in the sizes of cellulose hydrogels prepared by heating and freezing processes, where relatively smaller pores were observed after heating treatment (Chang et al., 2010). It was explained that the freezing method allowed for slow but strong self-association of cellulose chains at low temperature (Chang et al., 2010). Therefore, less shrinkage occurred during freeze-drying. It was also noticed that small fibers remained in the beads, suggesting the incomplete dissolution of waste office paper in NaOH/urea aqueous solution. Even though office paper was pre-treated by acid hydrolysis, the average molecular weight of cellulose may have been still high. Similar phenomenon was observed in spruce cellulose/NaOH/urea aqueous suspensions (Gong et al., 2014). Hydrolyzed spruce cellulose samples were partially dissolved and could form gels easily (Gong et al., 2014). A porous ‘matrix-filler’ network structure was constructed in which the dissolved cellulose was physically crosslinked and regenerated to form a three-dimensional hydrogel network, and the undissolved cellulose fibers acted as fillers to support the hydrogel structure. After loading the fertilizer, the porous structure of cellulose beads became dense (Figs. 4.4e and 4.4g), and the fertilizer particles were clearly distinguished on the surface of cellulose fibers (Figs. 4.4f and 4.4h), suggesting that the fertilizer was successfully trapped in the three-dimensional hydrogel network.

Table 4.1 Re-swelling ratio and amount of fertilizer loaded in freeze dried and oven dried cellulose beads.

Samples	**Re-swelling ratio / %**	**Fertilizer loaded in beads / mg/g**
Freeze dried beads	415.62±18.13	143.3±8.52
Oven dried beads	224.16±5.51	127.9±2.56

The re-swelling ratios of dry cellulose beads (FE & OE) were measured to evaluate their capacity to absorb water, and the values are listed in Table 4.1. Both FE and OE were able to uptake a certain amount of water, which was attributed to the well-maintained porous structure of cellulose hydrogel beads. The re-welling ratio of FE beads (415.62±18.13 %) was considerably higher than that of OE beads (224.16±5.51%), when compared by a percent ratio FE beads could uphold 185.4% more water than OE beads. This could further be explained by the larger pores of FE as observed in SEM images. Consequently, a stronger water retention capacity could be expected for FE beads. The amount of fertilizer loaded in the cellulose hydrogel beads (FD &OD)

was also calculated by monitoring the weight change before and after washing, because the fertilizer is composed of inorganic compounds and can be fully dissolved in water. However, the calculated values for OD and FD were 878.53±92.2 mg/g and 102.12 ±10.1 mg/g, respectively. It meant that, compared to FD sample, a larger weight loss occurred in OD beads during washing. Considering the same concentration (10% w/v) of fertilizer solution used for loading, this large weight loss of OD should not be completely due to the removal of fertilizer in the beads, and some parts of cellulose hydrogels might also be washed away. It suggested that OD beads might not be as stable as FD sample, and more importantly, it was not suitable to calculate the amount of fertilizer by this gravimetric method. Therefore, the amounts of nitrogen, phosphorus and potassium (N-P-K) nutrients released from FD and OD were determined through atomic absorption elemental analysis. The release behavior of commercial fertilizer granules was tested and compared. As shown in Fig.4.5, the amounts of released N-P-K were: FD (N: 56.8 ±3.92 mg/g, P: 49.7±3.82 mg/g and K: 36.8±1.38 mg/g), OD (N: 49.7±0.726 mg/g, P: 44.1±1.70 mg/g and K: 34.1±1.11 mg/g), and commercial fertilizer granules (N: 122.2±4.04 mg/g, P: 104.1±1.60 mg/g and K: 79.7±2.34 mg/g). It was worth noting that the ratios of N-P-K released from the regenerated cellulose hydrogel beads were quite similar to that from commercial fertilizer. It indicated that both cellulose hydrogel matrices prepared by two drying methods did not have a specific absorption towards any of the N-P-K salts, nor did they change the composition of fertilizer. According to the above results, it was calculated that the amount of fertilizer loaded in FD (143.3 ±8.52 mg/g) was slightly higher than that in OD (127.9 ±2.56 mg/g). It could also be explained by the larger pores of freeze-dried cellulose hydrogel beads. Although the released N-P-K from FD and OD were noticeably less than that from commercial fertilizer granules, it was because of the relatively low concentration of fertilizer solution used for loading. Consequently, this could be improved by simply increasing the content of fertilizer in the soaking bath.

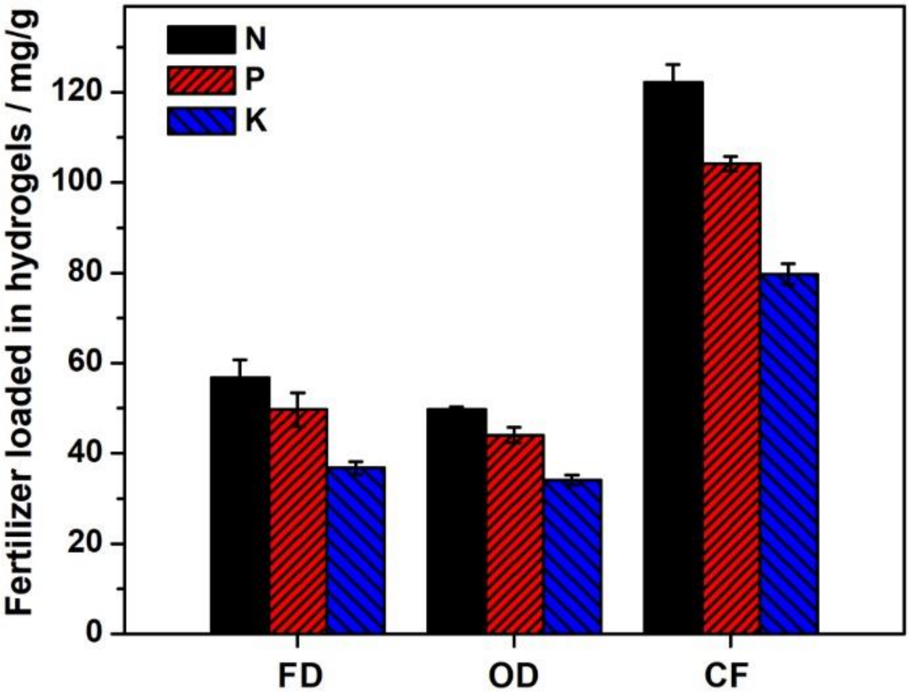

Figure 4.5 Atomic absorption elemental analysis of N-P-K nutrients released from freeze dried cellulose beads (FD), oven dried cellulose beads (OD), and commercial fertilizer (CF) with the standard deviations represented as error bars; for the analysis was done as true triplicates.

4.5 Conclusion

Cellulose hydrogel beads with uniform shape and porous structure were successfully prepared from waste office paper through a “green” NaOH/urea aqueous solvent system. Waste office paper was pre-treated by sulfuric acid hydrolysis to decrease the molecular weight of cellulose, and then partially dissolved in NaOH/urea aqueous solution in 15 min at -12.6 $_{o}$C. Cellulose hydrogel beads were regenerated in acid bath, and a porous ‘matrix-filler’ network structure was constructed in which the dissolved cellulose was physically crosslinked and regenerated to form a three-dimensional hydrogel network, and the undissolved cellulose fibers acted as fillers to support the hydrogel structure. During the dissolution and regeneration, the crystalline structure of cellulose changed from cellulose type I to cellulose type II. Commercial fertilizer was loaded in cellulose hydrogel beads, and dried through oven drying and freeze-drying. Fertilizer was kept in the porous structure and attached to the surface of cellulose fibers, but did not affect the morphology of cellulose beads. However, the freeze-drying process resulted in cellulose beads with larger pores and overall size compared to oven-dried beads. Consequently, the freeze-dried cellulose beads exhibited a higher re-swelling ratio and slightly larger amount of loaded fertilizer, which might be of benefit to provide nutrients and reserve water in dry soil. The loading of fertilizer in cellulose hydrogel beads did not affect the ratio of N-P-K, and further field experiment will be carried out to evaluate their performance in promoting the growth of plants.

Chapter 5. General Conclusion and Recommendations for Future Work

In the present research, sulfuric acid and NaOH/urea aqueous solvent systems were applied to recycle waste paper into biodegradable functional materials. An emphasis was given to the potential applications of resultant materials in active food packaging and agriculture.

First, waste office paper and cardboard were successfully dissolved in concentrated sulfuric acid aqueous solvent, and then regenerated into cellulose films that were loaded with active compounds (ZnO and carvacrol essential oil) to display antimicrobial activity against gram-positive and gram-negative bacteria. The dissolution process was visualized by optical microscopy, where cellulose fibers gradually swelled and disappeared in 210 s. The dissolution of waste cardboard was relatively slower than that of office paper, and several tiny undissolved pieces of cardboard were observed in the solution, which might be attributed to its high lignin content. After dissolution and regeneration, the crystalline structure of cellulose changed from cellulose type I to cellulose type II. Transparent and uniform films were obtained from waste office paper, which exhibited the similar mechanical properties compared to those of cellulose films prepared from spruce pulp in the same solvent. Therefore, it overcame the challenge in recycling waste paper caused by the shortening of cellulose fibers. The films regenerated from waste cardboard displayed a UV-light barrier property due to the lignin residues present. It was worth noting that the tensile strength and Young's modulus of regenerated cellulose films were comparable to those of some synthetic plastics. It suggested the potential to partially replace the non-biodegradable synthetic plastic food packaging in the future.

Secondly, cellulose hydrogel beads with uniform shape and porous structure were successfully prepared from waste office paper through a “green” NaOH/urea aqueous solvent system. Waste office paper was pre-treated by sulfuric acid hydrolysis to decrease the molecular weight of cellulose, and then partially dissolved in NaOH/urea aqueous solution in 15 min at -12.6 $_o$C. Cellulose hydrogel beads were regenerated in acid bath, and a porous ‘matrix-filler’ network structure was constructed in which the dissolved cellulose was physically crosslinked and regenerated to form a three-dimensional hydrogel network, and the undissolved cellulose fibers acted as fillers to support the hydrogel structure. During the dissolution and regeneration, the crystalline structure of cellulose changed from cellulose type I to cellulose type II. Commercial fertilizer was loaded in cellulose hydrogel beads, and dried through oven drying and freeze-drying. Fertilizer was kept in the porous structure and attached to the surface of cellulose fibers, but did not affect the morphology of cellulose beads. However, the freeze-drying process resulted in cellulose beads with larger pores and overall size compared to oven-dried beads. Consequently, the freeze-dried cellulose beads exhibited a higher re-swelling ratio and slightly larger amount of loaded fertilizer, which might be of benefit to provide nutrients and reserve water in dry soil. The loading of fertilizer in cellulose hydrogel beads did not affect the ratio of N-P-K, and further field experiment will be carried out to evaluate their performance in promoting the growth of plants.

Overall, waste paper is a promising source to generate cellulose-based biodegradable materials, and the “green” aqueous solvent systems are effective to convert cellulosic waste into various forms of materials.

Based on the findings in this thesis, several recommendations for future research were identified as follow:

- Molecular weight of cellulose in waste materials should be determined to better control the quality and properties of regenerated cellulose films and hydrogels.
- The contents of lignin and other inorganic additives in waste paper and regenerated cellulose materials should be determined to better understand their properties and assess the safety issue for food related applications.
- Optimization of antimicrobial active compound (i.e. ZnO and carvacrol essential oil) contents in regenerated cellulose films to achieve the best inhibition effect as active food packaging materials.
- The performance of cellulose-based antimicrobial films as active packaging of food products, such as fruits, vegetables and meats, should be evaluated.
- Optimization of the extent of pre-hydrolysis to determine the best condition for the dissolution of waste paper in NaOH/urea aqueous solvent.
- Optimization of the amount of fertilizer loaded in regenerated cellulose hydrogel beads and determination of release behavior of fertilizer in water and soil.
- The effect of regenerated cellulose beads loaded with fertilizer on the growth of plants in dry land should be studied to determine their performance in real applications.

References

Ahmad, N. A., Mohd Kaus, N. H., Khan, I., Haafiz, M., & Kassim, M. (2018). Relationship between dissolution temperature and properties of oil palm biomass based-regenerated cellulose films prepared via ionic liquid. *Materials Chemistry and Physics, 221,* 382-389.

Alves, L., Medronho, B. F., Antunes, F. E., Romano, A., Miguel, M. G., & Lindman, B. (2015). On the role of hydrophobic interactions in cellulose dissolution and regeneration: Colloidal aggregates and molecular solutions. *Colloids and Surfaces A: Physicochemical and Engineering Aspects, 483,* 257-263.

Alves, L., Medronho, B., Antunes, F. E., Topgaard, D., & Lindman, B. (2016). Dissolution state of cellulose in aqueous systems. 1. Alkaline solvents. *Cellulose, 23*, 247-258.

Annamalai, N., Battashi, H. A., Anu, S. N., Azkawi, A. A., Bahry, S. A., & Sivakumar, N. (2020). Enhanced bioethanol production from waste paper through separate hydrolysis and fermentation. *Waste and Biomass Valorization, 11*, 121-131.

Annamalai, N., Sivakumar, N., & Oleskowicz-Popiel, P. (2018). Enhanced production of microbial lipids from waste office paper by the oleaginous yeast Cryptococcus curvatus. *Fuel, 217*, 420-426.

Bajpai, P. (2017). Chapter 3 - Structure and Properties of Cellulose and Nanocellulose. In P. Bajpai (Ed.), *Pulp and Paper Industry* (pp. 27-40): Elsevier.

Cai J. & Zhang L. (2006). Unique gelation behavior of cellulose in NaOH/urea aqueous solution, *Biomacromolecules, 7,* 183–189.

Cai J. & Zhang L.(2005). Rapid dissolution of cellulose in LiOH/urea and NaOH/urea aqueous solutions. *Macromolecular Bioscience, 5,* 539–548.

Cai J., Zhang L., Chang C., Cheng G., Chen X. & Chu B. (2007). Hydrogen-bond-induced inclusion complex in aqueous cellulose/LiOH/urea solution at low temperature, *Chemical Physics and Physical Chemistry, 8,* 1572–1579.

Cai J., Zhang L., Liu S., Liu Y., Xu X., Chen X., Chu B., Guo X., Xu J., Cheng H., Han C. C. & Kuga, S. (2008). Dynamic self-assembly induced rapid dissolution of cellulose at low temperatures. *Macromolecules, 41*, 9345–9351.

Calcagnile, P., Sibillano, T., Giannini, C., Sannino, A., & Demitri, C. (2019). Biodegradable poly(lactic acid)/cellulose-based superabsorbent hydrogel composite material as water and fertilizer reservoir in agricultural applications. *Journal of Applied Polymer Science, 136,* 47546.

Carrick, C., Lindstrom, S. B., Larsson, P. T., & Wagberg, L. (2014). Lightweight, highly compressible, noncrystalline cellulose capsules. *Langmuir, 30*, 7635-7644.

Causin, V., Marega, C., Marigo, A., Casamassima, R., Peluso, G., & Ripani, L. (2010). Forensic differentialtion of paper by X-ray diffraction and infrared spectroscopy. *Forensic Science International, 197,* 70-74.

Chang, C., Zhang, L., Zhou, J., Zhang, L., & Kennedy, J. F. (2010). Structure and properties of hydrogels prepared from cellulose in NaOH/urea aqueous solutions. *Carbohydrate Polymers, 82*, 122-127.

Chen, X., Chen, X., Cai, X. M., Huang, S., & Wang, F. (2018). Cellulose dissolution in a mixed solvent of tetra(n-butyl)ammonium hydroxide/dimethyl sulfoxide via radical reactions. *American Chemical Society Sustainable Chemistry & Engineering, 6*, 2898-2904.

Chen, Y., Lu, W., Guo, Y., Zhu, Y., & Song, Y. (2019). Electrospun gelatin fibers surface loaded ZnO particles as a potential biodegradable antibacterial wound dressing. *Nanomaterials, 9,* 525.

Cook, M. T., Tzortzis, G., Charalampopoulos, D. & Khutoryanskiy, V. V. (2012). Microencapsulation of probiotics for gastro-intestinal delivery. *Journal of Controlled Release, 162*, 56-67.

Cuce, E., Cuce, P., Wood, C. J. & Riffat, S. B. (2014). Toward aerogel based thermal superinsulation in buildings: A comprehensive review. *Renewable Sustainable Energy Rev, 34*, 273-299.

Cuissinat, C., & Navard, P. (2006). Swelling and dissolution of cellulose part 1: free floating cotton and wood fibres in N-methylmorpholine-N-oxide-water mixtures. *Macromolecular Symposia, 244*, 1-18.

Dashipour, A., Razavilar, V., Hosseini, H., Shojaee-Aliabadi, S., German, J. B., Ghanati, K., Khakpour, M., & Khaksar, R. (2015). Antioxidant and antimicrobial carboxymethyl cellulose films containing Zataria multiflora essential oil. *International Journal of Biological Macromolecules, 72*, 606-613.

Dubey, A. K., Gupta, P. K., Garg, N., & Naithani, S. (2012). Bioethanol production from wastepaper acid pretreated hydrolyzate with xylose fermenting Pichia stipitis. *Carbohydrate Polymers, 88,* 825-829.

El-Sakhawy, M., & Hassan, M. (2007). Physical and mechanical properties of microcrystalline cellulose prepared from agricultural residues. *Carbohydrate Polymers, 67*, 1-10.

FAO.(2018). FAOSTAT: Forestry Production and Trade. Retrieved from http://www.fao.org/faostat/en/#data/FO. Retrieved Mai 26, 2020

Freudenberg K (1936) The kinetics of long chain disintegration applied to cellulose and starch. *Transactions of the Faraday Society 32*, 74-75.

Fu, F., Gu, J., Xu, X., Xiong, Q., Zhang, Y., Liu, X., & Zhou, J. (2017). Interfacial assembly of ZnO–cellulose nanocomposite films via a solution process: a one-step biomimetic approach and excellent photocatalytic properties. *Cellulose, 24*, 147-162.

Fu, F., Li, L., Liu, L., Cai, J., Zhang, Y., Zhou, J., & Zhang, L. (2015). Construction of cellulose based ZnO nanocomposite films with antibacterial properties through one-step coagulation. *American Chemical Society Applied Materials & Interfaces*, *7,* 2597-2606.

Genga, H., Yuana, Z., Fana, Q., Daia, X., Zhaoa, Y., Wanga, Z., & Qin, M. (2014). Characterisation of cellulose films regenerated from acetone/water coagulants.*Carbohydrate Polymers*, *102*, 438-444.

Gong, X., Wang, Y., Tian, Z., Zheng, X., & Chen, L. (2014). Controlled production of spruce cellulose gels using an environmentally ‘‘green’’ system. *Cellulose*, *21*, 1667-1678.

Han, Y., Zhang, X., Wu, X., & Lu, C. (2015). Flame retardant, heat insulating cellulose aerogels from waste cotton fabrics by in situ formation of magnesium hydroxide nanoparticles in cellulose gel nanostructures. *American Chemical Society Sustainable Chemistry &. Engineering, 3,* 1853-1859.

Huang, W., Wang, Y., Zhang, L., & Chen, L. (2016). Rapid dissolution of spruce cellulose in H_2SO_4 aqueous solution at low temperature. *Cellulose, 23*, 3463-3473.

Jiang, Z., Fang, Y., Ma, Y., Liu, M., Liu, R., Guo, H., Lu, A. & Zhang, L. (2017). Dissolution and metastable solution of cellulose in NaOH/thiourea at 8 °C for construction of nanofibers. *Journal of Physical Chem. B, 121*, 1793-1801.

Jiang, Z., Fang, Y., Xiang, J., Ma, Y., Lu, A., Kang, H., .. & Zhang, L. (2014). Intermolecular interactions and 3D structure in cellulose-NaOH-urea aqueous system. *Journal of Physical Chem B, 118,* 10250-10257.

Joshi, G., Naithani, S., Varshney, V. K., Bisht, S. S., Rana, V., & Gupta, P. K. (2015). Synthesis and characterization of carboxymethyl cellulose from office waste paper: A greener approach towards waste management. *Waste Management. 38*, 33-40.

Kafle, K., Greeson, K., Lee, C., & Kim, S. H. (2014). Cellulose polymorphs and physical properties of cotton fabrics processed with commercial textile mills for mercerization and liquid ammonia treatments. *Textile Research Journal, 84*, 1692-1699.

Kallos, E., & Apostolopoulou, T. (2020). Cellulosic Ethanol and the future of Biofuels: From carbohydrates to hydrocarbons. *Scientific Figure on ResearchGate*. Available from: https://www.researchgate.net/figure/Cellulose-Molecules_fig12_242113626 [accessed 20 May, 2020]

Kim, S. S., Jeong, J., & Lee, J. (2014). Antimicrobial m-aramid/cellulose blend membranes for water disinfection. *Industrial & Engineering Chemistry Research, 53*, 1638-1644.

Kirby, W. M., Yoshihara, G. M., Sundsted, K. S., & Warren, J. H. (1956-1957). Clinical usefulness of a single disc method for antibiotic sensitivity testing. *Antibiotics annual*, 892-897.

Klemm, D., Philipp, B., Heinze, T., Heinze, U., & Wagenknecht, W. (1998). Comprehensive Cellulose Chemistry. Volume 1. Fundamentals and analytical methods. *Journal of the American Chemical Society*, 121, 8677.

Landín, M., Martínez-Pacheco, R., Gómez-Amoza, J. L., Souto, C., Concheiro, A., & Rowe, R. C. (1993). Effect of batch variation and source of pulp on the properties of microcrystalline cellulose. *International Journal of Pharmaceutics. 91*, 133-141.

Lei, W.Q., Fang, C.Q., Zhou, X.,Yin, Q., Pan, S.F., Yang, R., Liu, D.H. & Ouyang, Y (2018). Cellulose nanocrystals obtained from office waste paper and their potential application in PET packing materials. *Carbohydrate Polymers. 181*, 376-385.

Li, J., Zhu, Z., Li, T., Peng, X., Jiang, S., & Turng, L. S. (2019). Quantification of the Young's modulus for polypropylene: Influence of initial crystallinity and service temperature. *Journal of Applied Polymer Science*, *137*, 48581.

Li, L., Li, B., Sun, H., & Zhang, J. (2017). Compressible and conductive carbon aerogels from waste paper with exceptional performance for oil/water separation. *Journal of Materials Chemistry A, 5*, 14858-14864.

Li, R., Wang, S., Lu, A., & Zhang, L. (2015). Dissolution of cellulose from different sources in an NaOH/urea aqueous system at low temperature. *Cellulose, 22*, 339-349.

Li, Y., Xiao, H., Pan, Y., & Wang, L. (2018). Novel composite adsorbent consisting of dissolved cellulose fiber/microfibrillated cellulose for dye removal from aqueous solution. *American Chemical Society Sustainable Chemistry &. Engineering*, *6,* 6994-7002.

Li, Z., Shao, L., Ruan, Z., Hu, W., Lu, L., & Chen, Y. (2018). Converting untreated waste office paper and chitosan into aerogel adsorbent for the removal of heavy metal ions. *Carbohydrate Polymers, 193*, 221-227.

Li, L., Li, B., Sun, H., & Zhang, J. (2017). Compressible and conductive carbon aerogelsfrom wastepaper with exceptional performance for oil/water separation. *Journal of Material Chemistry A*, *5*, 14858-14864.

Liu, P., Guo, X., Nan, F., Duan, Y., & Zhang, J. (2016). Modifying mechanical, optical properties and thermal processability of iridescent cellulose nanocrystal films using ionic liquid. *ACS Applied Materials & Interfaces, 9,* 3085-3092.

Luan, Q., Zhou, W., Zhang, H., Bao, Y., Zheng, M., Shi, J., Tang, H. & Huang, F. (2018). Cellulose-based composite macrogels from cellulose fiber and cellulose nanofiber as intestine delivery vehicles for probiotics. *Journal of Agricultural and Food Chemistry, 66*, 339-345.

Lue A. & Zhang L. (2008). Investigation of the scaling law on cellulose solution prepared at low temperature. *Journal of Physical Chem B, 112,* 4488-4495.

Lue A., Zhang L. & Ruan D. (2007). Inclusion complex formation of cellulose in NaOH-thiourea aqueous system at low temperature, *Macromolecular Chemistry and Physics, 208,* 2359-2366.

Ma, H., Zhang, F., Li, Q., Chen, G., Hub, S., & Cheng, H. (2019). Preparation of ZnO nanoparticle loaded amidoximated wool fibers as a promising antibiofouling adsorbent for uranium(VI) recovery. *RSC Advances, 9*, 18406-18414.

Ma, Y., Hummel, M., Määttänen, M., Särkilahti, A., Harlin, A., & Sixta, H. (2016). Upcycling of waste paper and cardboard to textiles. *Green Chemistry, 18,* 858-866.

Marzuki, N. H., Irfiania, N., Wahit, M. U., Othman, N., & Yusoff, N. I. S. M. (2018). Mechanical properties of kenaf fiber and montmorillonite reinforced recycled polyethylene terephthalate/recycled polypropylene. *Materialstoday: Proceedings, 5,* 21879-21887.

Medronho, B., & Lindman, B. (2014). Competing forces during cellulose dissolution: From solvents to mechanisms. *Current Opinion in Colloid Interface Science*, *19*, 32-40.

Medronho, B., & Lindman, B. (2015). Brief overview on cellulose dissolution/regeneration interactions and mechanisms. *Advances in Colloid and Interface Science*, *222*, 502-508.

Medronho, B., Romano, A., Miguel, M. G., Stigsson, L., & Lindman, B. (2012). Rationalizing cellulose (in)solubility: reviewing basic physicochemical aspects and role of hydrophobic interactions. *Cellulose, 19*, 581-587.

Mikkonen, K. S., Parikka, K., Ghafar, A., & Tenkanen, M. (2013). Prospects of polysaccharide aerogels as modern advanced food materials. *Trends in Food Science & Technology, 34*, 124-136.

Minnick, D. L., Flores, R. A., DeStefano, M. R., & Scurto, A. M. (2016). Cellulose solubility in ionic liquid mixtures: Temperature, cosolvent,and antisolvent effects *Journal of Physical Chem B*, *32*, 7906-7919.

Nakasone, K., Ikematsu, S., & Kobayashi, T. (2016). Biocompatibility evaluation of cellulose hydrogel film regenerated from sugar cane bagasse waste and its in vivo behavior in mice. *Industrial & Engineering Chemistry Research*, *55*, 30-37.

Neelamegam, A., Al-Battashi, H., Al-Bahry, S., & Nallusamy, S. (2018). Biorefinery production of poly-3-hydroxybutyrate using waste office paper hydrolysate as feedstock for microbial fermentation. *Journal of Biotechnology, 265*, 25-30.

Nishiwaki-Akine, Y., Kanazawa, S., Uneyama, T., Nitta, K., Yamamoto-Ikemoto, R., & Watanabe, T. (2017). Transparent woody film made by dissolution of finely divided Japanese Beech in formic acid at room temperature. *American Chemical Society Sustainable Chemistry &. Engineering, 5*, 11536-11542.

Oh, S. Y., Yoo, D. I., Shin, Y., & Seo, G. (2005). FTIR analysis of cellulose treated with sodium hydroxide and carbon dioxide. *Carbohydrate Research, 340*, 417-428.

Olsson, C., & Westman, G. (2013). Direct Dissolution of Cellulose: Background, Means and Applications. *Cellulose-Fundamental Aspects, 6,* 143-178.

Omura, T., Imagawa, K., Kono, K., Suzuki, T., & Minami, H. (2017). Encapsulation of either hydrophilic or hydrophobic substances in spongy cellulose particles. *American Chemical Society Applied Materials & Interfaces. 9*, 944-949.

Orue, A., Santamaria-Echart, A., Eceiza, A., Peña-Rodriguez, C., & Arbelaiz, A. (2017). Office waste paper as cellulose nanocrystal source. *Journal of Applied Polymer Science, 134*, 45257.

Palange, C., Johns, M. A., Scurr, D. J., Phipps, J. S., & Eichhorn, S. J. (2019). The effect of the dispersion of microfibrillated cellulose on the mechanical properties of melt-compounded polypropylene-polyethylene copolymer. *Cellulose, 26*, 9645-9659.

Parkinson, & Allen. (1975). A wet oxidation procedure suitable for the determination of nitrogen and mineral nutrients in biological material. *Communication in Soil Science and Plant Analysis, 6*, 1-11.

Sadeghifar, H., Venditti, R., Jur, J., Gorga, R. E., & Pawlak, J. J. (2017). Cellulose-lignin biodegradable and flexible UV protection film. *American Chemical Society Sustainable Chemistry &. Engineering. 5*, 625-631.

Saito, T., Kimura, S., Nishiyama, Y. & Isogai, A. (2007). Cellulose nanofibers prepared by TEMPO-mediated oxidation of native cellulose. *Biomacromolecules, 8,* 2485-2491.

Shitole, A. A., Raut, P. W., Sharma, N., Giram, P., Khandwekar, A. P., & Garnaik, B. (2019). Electrospun polycaprolactone/hydroxyapatite/ZnO nanofibers as potential biomaterials for bone tissue regeneration. *Journal of Materials Science: Materials in Medicine, 30*, 51.

Sjöström, E. (1993). Chapter 9 – Cellulose derivatives. In E. Sjöström (Ed.), *Wood Chemistry (Second Edition)* (pp. 204-224). San Diego: Academic Press.

Soo Kim, S., Lee, J., & Jeong, J. (2014). Antimicrobial m-Aramid/Cellulose blend membranes for water disinfection. *Industrial & Engineering Chemistry Research, 53,* 1638-1644.

Sundberg, J., Guccini, V., Håkansson, K. M. O., Salazar-Alvarez, G., Toriz, G., & Gatenholm, P. (2015). Controlled molecular reorientation enables strong cellulose fibers regenerated from ionic liquid solutions. *Polymer, 75,* 119-124.

Thoorens, G., Krier, F., Leclercq, B., Carlin, B., & Evrard, B. (2014). Microcrystalline cellulose, a direct compression binder in a quality by design environment:A review. *International Journal of Pharmaceutics, 473,* 64-72.

Tunç,S., & Duman,O., (2011).Preparation of active antimicrobial methylcellulose / carvacrol / montmorllonite nanocomposite films and investigation of carvacrol release. *LWT - Food Science and Technology, 44*, 465-472.

Uesu, N. Y., Pineda, E. A., & Hechenleitner, A. A. (2000). Microcrystalline cellulose from soybean husk: Effects of solvent treatments on its properties as acetylsalicylic acid carrier. *International Journal of Pharmaceutics, 206*, 85-96.

Wang, C., Shi, J., He, M., Ding, L., Li, S., Wang, Z., & Wei, J. (2018). High strength cellulose/ATT composite films with good oxygen barrier property for sustainable packaging applications. *Cellulose, 25,* 4145-4154.

Wang, Q., Wang, Y., Chen, L., Cai, J., & Zhang, L. (2017). Facile construction of cellulose nanocomposite aerogel containing TiO2 nanoparticles with high content and small size and their applications. *Cellulose, 24*, 2229-2240.

Wang, W., Yang, S., Zhang, A., & Yang, Z. (2020). Preparation and properties of novel corn straw cellulose-based superabsorbent with wate-retaining and slow-release functions. *Journal of Applied Polymer Science, 137,* 48951.

Wang, Y., & Chen, L. (2011). Impacts of nanowhisker on formation kinetics and properties of all-cellulose composite gels. *Carbohydrate Polymers, 83*, 1937-1946.

Wei, W., Meng, F., Cui, Y., Jiang, M., & Zhou, Z. (2017). Room temperature dissolution of cellulose in tetra-butylammonium hydroxide aqueous solvent through adjustment of solvent amphiphilicity. *Cellulose, 24*, 49-59.

Wittmar, A. S. M., Fu, Q., & Ulbricht, M. (2017). Photocatalytic and magnetic porous cellulose-based nanocomposite films prepared by a green method. *American Chemical Society Sustainable Chemistry &. Engineering, 5*, 9858-9868.

Yan, L., Wang, L., Gao, S., Liu, C., Zhang, Z., Ma, A., & Zheng, L. (2020). Celery cellulose hydrogel as carriers for controlled release of short-chain fatty acid by ultrasound. *Food Chemistry, 309*, 125717.

Yohana, C., A., Sriwidodo, S., & Abdassah, M. (2019). Chapter: Microcrystalline cellulose as pharmaceutical excipient. *Pharmaceutical Formulation Design - Recent Practices*.
DOI: 10.5772/intechopen.88092.

Zhang, H., Yang, M., Luan, Q., Tang, H., Huang, F., Xiang, X., Yang, C. & Bao, Y. (2017). Cellulose anionic hydrogels based on cellulose nanofibers as natural stimulants for seed germination and seedling growth. *Journal of Agricultural and Food Chemistry, 65*, 3785-3791.

Zhang, J., Luo, N., Wan, J., Xia, G., Yu, J., He, J., & Zhang, J. (2017). Directly converting agricultural straw into all-biomass nanocomposite films reinforced with additional in situ-retained cellulose nanocrystals. *American Chemical Society Sustainable Chemistry &. Engineering, Eng. 5*, 5127-5133.

Zhang, L. Q., Niu, B., Yang, S. G., Huang, H. D., Gan-Ji Zhong, G. J., & Li, Z. M. (2016). Simultaneous preparation and dispersion of regenerated cellulose nanoparticles using a facile protocol of dissolution−gelation− isolation−melt extrusion. *American Chemical Society Sustainable Chemistry &. Engineering, 4*, 2470-2478.

Zhang, Z., Macquarrie, D. J., De Bruyn, M., Budarin, V. L., Hunt, A. J., Gronnow, M. J., Fan, J., Shuttleworth, P. S., Clark, J. H., & Matharu, A. S. (2015). Low-temperature microwave-assisted pyrolysis of waste office paper and the application of bio-oil as an Al adhesive. *Green Chemistry, 17*, 260-270.

Zhao, J., Lu, Z., He, X., Zhang, X., Li, Q., Xia, T., Zhang, W. & Lu, C. (2017). Fabrication and characterization of highly porous Fe(OH)3@cellulose hybrid fibers for effective removal of congo red from contaminated water. *American Chemical Society Sustainable Chemistry &. Engineering, 5*, 7723-7732.

Zhou, J., Chang, C., Zhang, R., & Zhang, L. (2007). Hydrogels prepared from unsubstituted cellulose in NaOH/Urea aqueous solution. *Macromolecular Bioscience,7*, 804-809.